



POLITECNICO MILANO 1863

Space Systems Engineering and Operations

AA 2023-2024

Professor: Michèle Roberta Lavagna

OSTM/Jason-2 Mission

A Reverse Engineering Exercise

Group 25

Person Code	Surname	Name
10726898	Juvara	Matteo Giovanni
10717230	Beretta	Beatrice
10705062	Nicolucci	Edoardo
10973691	Separovic	Marko Tomislav
10735389	Orsenigo	Samuele
10728962	Modelli	Simone

July 19, 2024

Contents

1 System Overview & Mission Analysis	10
1.1 Mission Overview	10
1.2 Mission Main Goals	10
1.3 Mission Drivers	10
1.4 Functional Analysis	11
1.5 Mission Phases & ConOps	11
1.5.1 Launch Sequence	12
1.5.2 Extended Phase	12
1.6 Scientific Instruments	13
1.6.1 Overview	13
1.6.2 Payload Description	13
1.6.3 Main Goals - P/L correlations	15
1.6.4 ConOps - P/L correlations	15
1.7 Mission Analysis	15
1.7.1 Nominal Orbit	15
1.7.2 Orbits History & Phase Correlation	16
1.7.3 Orbit maintenance	16
2 Mission Analysis & Propulsion Subsystem	17
2.1 Mission Analysis	17
2.1.1 Orbit Choice	17
2.1.2 ΔV Estimation	17
2.1.3 Launcher Selection	18
2.1.4 Orbit Acquisition	18
2.1.5 Station Keeping	19
2.1.6 Margins and Comparison	19
2.2 Propulsion System	19
2.2.1 Propulsion System Overview	19
2.3 Propulsion System Sizing and Analysis	20
2.3.1 Propellant Selection and Masses	21
2.3.2 Tank Sizing and Masses	21
2.3.3 Feeding Lines	22
2.3.4 Thrusters	23
3 Tracking Telemetry & Telecommand Subsystem	24
3.1 Architecture and Design	25
3.1.1 Ground Segment Architecture	25
3.1.2 Signal Elaboration and TTMTA Architecture	25
3.1.3 Signal Selection	26
3.2 Modes and Mission Phases	26
3.2.1 Initial Requirements	27
3.2.2 Satellite Active Modes	27
3.3 Reverse Sizing	28
3.3.1 Losses	28
3.3.2 Antennas	28
3.3.3 Amplifier	29
3.3.4 Link Budget	29

4 Attitude Dynamics and Control Subsystem	30
4.1 Architecture	30
4.1.1 Sensors	31
4.1.2 Actuators	32
4.2 Control modes	32
4.3 Pointing Budget	33
4.4 Disturbances	34
4.5 Reverse Sizing	36
4.5.1 Reaction Wheels	36
4.5.2 Thrusters	36
5 Thermal Control Subsystem	38
5.1 Architecture	38
5.1.1 Multi Layer Insulation (MLI)	39
5.1.2 Heater Lines and Thermistors	39
5.1.3 Silvered SSM Radiators	39
5.1.4 Thermal Straps and Insulating Washers	40
5.2 Design Choices	40
5.2.1 Constraints	40
5.2.2 Requirements and Objectives	40
5.3 Environment and Temperature Range	41
5.3.1 Environment	41
5.3.2 Temperature Ranges	41
5.4 Reverse Sizing	42
5.4.1 Thermal heat sources	42
5.4.2 Spacecraft Modelling	42
6 Electrical Power Subsystem	44
6.1 Architecture	44
6.1.1 EPS Components	44
6.1.2 Battery Management	45
6.2 Power Budget and phase analysis	46
6.3 Reverse Sizing	46
6.3.1 Introduction	46
6.3.2 Establishing Initial Parameters	46
6.3.3 Calculation and sizing	47
7 Configuration System & On-Board Data Handling	50
7.1 Configuration System	50
7.1.1 Vehicle Shape and Interface with Launcher Fairing	50
7.1.2 External Surface design	51
7.1.3 Internal design	52
7.2 On-Board Data Handling	53
7.2.1 Architecture	53
7.2.2 Reverse Sizing	54
7.2.3 Conclusions	56

List of Figures

1.1	Functional Tree Analysis	11
1.2	Mission Phase & ConOps	12
1.3	Jason-2 Official Launch Sequence	12
1.4	Payloads on board of Jason-2	15
1.5	3D Ground Track for a 10-day cycle [3]	15
1.6	Single Orbit Plot	16
1.7	2D Ground Track for a 10 day cycle	16
2.1	2D Ground Track for a 10 day cycle	17
2.2	Achievable orbits vs launch sites and vehicles	18
2.3	Orbital acquisition strategy	19
2.4	Schematic of PROTEUS's Propulsion System	20
2.5	PROTEUS internal view [11]	21
2.6	1N Thrusters schematic [1]	23
3.1	Jason 2 System Architecture	25
3.2	Ground Stations	25
3.3	PROTEUS Data Path Scheme	25
3.4	PROTEUS Telemetry Scheme	25
3.5	Jason-2's Phases [26]	27
4.1	Proteus Platform Exploded Assembly Drawing	30
4.2	3D illustration of Jason2's attitude determination by PRESTO	31
4.3	Yaw steering correction for solar panels	31
4.4	Pointing Performances in the extended phase	34
5.1	TCS Components' Design	38
5.2	Interface PROTEUS - Payload	39
5.3	MLI Interface between Platform and Payload	39
5.4	Silvered SSM on Jason 2	40
5.5	Heat Exchanges between the Environment and the Spacecraft.	41
5.6	Proteus Platform's Temperature Ranges [42]	41
5.7	Payload Instruments' Temperature Ranges	41
6.1	EPS overall architecture	44
6.2	One wing of the SA on Jason-2	45
6.3	Battery Pack on Jason 2	45
7.1	General Satellite Architecture based on Proteus Bus	51
7.2	Jason 2 Launcher Configuration	51
7.3	Reference Frame of Jason 2 [26]	51
7.4	Instrument FOV Analysis	51
7.5	Back View of Jason 2	52
7.6	Bottom View of Jason 2	52
7.7	PROTEUS's internals photo	52
7.8	PROTEUS internal elements	52
7.9	Jason-2 payload internal elements	53
7.10	PROTEUS interface with Jason payload	53
7.11	On board computer system diagram	53

List of Tables

1.1	Science and Engineering goals [52]	10
1.2	Instrumentation Overview	13
1.3	Correlation between mission main goals and payloads	15
1.4	Correlation between mission phases and payloads	15
2.1	Mean classical orbit elements	17
2.2	Auxiliary Data	17
2.3	Launcher Data until 2011	18
2.4	Mass and Velocity Comparison	19
2.5	Comparison between the calculated data and the actual data [16]	22
3.1	Frequency couples reserved at UIT for PROTEUS	26
3.2	Technical Specifications for the largest dish of each Ground Station and Satellite	28
3.3	Uplink and downlink signal losses, transmitter and receiver gains [dB]	28
4.1	Sensor Data	32
4.2	Actuator Data	32
4.3	Hardware utilization in each mode [50].	33
4.4	Jason-2's pointing budget divided in subsystems for each phase and mode	34
4.5	Mean disturbance values	36
5.1	Thermo-optic characteristics of TCS components [26]	40
5.2	Areas and thermo-optic values of the main body[6]	42
5.3	Heat fluxes in the hot case	43
5.4	Heat fluxes in the cold case	43
6.1	Power Budget Analysis	46
6.2	Initial Data EPS	47
6.3	Solar Cells and Battery Data	47
6.4	Solar Panel Sizing and Comparizon	48
6.5	Battery Sizing and Comparizon	49
7.1	Redundancy of main processors[20]	54
7.2	Functions allocated to the OBDH Subsystem and typical throughputs	55
7.3	Final requirements for the processor	56

Acronyms

- ACS** Attitude Control Subsystem. 58
- ADCS** Attitude Dynamics and Control Subsystem. 11, 46, 55
- AMR** Advanced Microwave Radiometer. 13–15, 41, 46, 50, 51
- AOCS** Attitude and Orbit Control System. 30, 32–34
- BBQ** Barbecue Phase. 33
- BER** Bit Error Rate. 29
- BEU** Battery Electronic Unit. 45, 46
- BM** Battery Management. 45
- BOL** Beginning of Life. 45
- CARMEN-2** Environment Characterization and Modelisation 2. 13, 14, 46
- CCAFS** Cape Canaveral Air Force Station. 18
- CCSDS** Consultative Committee for Space Data Systems. 26
- CDAS** Command and Data Acquisition Stations. 28, 29, 57
- CNES** Centre National d’Études Spatiales. 10, 13, 25, 58
- ConOps** Concept of Operations. 4, 12
- CSS** Coarse Sun Sensor. 31–33
- DHU** Data Handling Unit. 25, 40, 44, 45, 52, 53
- DIODE** Détermination Immédiate d’Orbite par Doris Embarqué. 13
- DOD** Depth of Discharge. 47
- DORIS** Doppler Orbitography and Radiopositioning Integrated by Satellite. 13–15, 25, 41, 46, 51
- DTG** Dynamically Tuned Gyroscope. 31
- EOL** End of Life. 48
- EPS** Electrical Power Subsystem. 3, 6, 44, 47, 55
- ESA** Electronics Structure Assembly. 14
- ESA** European Space Agency. 19, 29, 48, 49, 58
- FOV** Field of View. 4, 27, 51
- GPS** Global Positioning System. 14, 25, 31–33, 51
- GPSP** Global Positioning System Payload. 13–15, 25, 46, 51
- GS** Ground Station. 28

GYR Gyro. 31–33

HKTM-P House Keeping Telemetry Pass. 27

HKTM-R House Keeping Telemetry Record. 27

iLRO Interleaved Long Repeat Orbit. 13, 16, 17, 19

JASON Joint Altimetry Satellite Oceanography Network. 10, 11, 13, 16, 25, 38

JAXA Japan Aerospace Exploration Agency. 13, 14

JMR Jason Microwave Radiometer. 14

JPL Jet Propulsion Laboratory. 13, 14, 58

LEO Low Earth Orbit. 19, 44

LEOP Launch and Early Orbit Phase. 20

LPT Light Particle Telescope. 13, 14, 46

LPT-E Light Particle Telescope Electronics. 14

LPT-S Light Particle Telescope Sensors. 14

LRA Laser Retroreflector Array. 13–15, 25, 51

LRO Long Repeat Orbit. 13, 16, 17, 19

LUM Launch Mode. 32, 33

MAG Magnetometer. 31–33

MEX Experiment Module. 14

MGA Medium Gain Antennas. 25, 28

MLI Multi Layer Insulation. 3, 4, 31, 38–41, 57

MTB Magnetic Torquer Bars. 33

NASA The National Aeronautics and Space Administration. 10–12, 58, 59

NOAA National Oceanic and Atmospheric Administration. 25, 28, 57, 58

NOM Nominal Mode. 33, 36, 46

OBDH On-Board Data Handling. 6, 46, 53–55

OBSW On Board Software. 45

OCM Orbit Control Mode. 19, 23, 33

OSCAR Observing Systems Capability Analysis and Review Tool. 13

OSTM Ocean Surface Topography Mission. 10, 11, 16, 17, 25, 31, 38

PCE Power Conditioning Equipment. 44–46, 55

PLTM Payload Telemetry. 27

POD Precise Orbit Determination. 13, 14, 25, 31, 50, 51, 59

POSEIDON Positioning,Ocean,Solid Earth, Ice Dynamics, Orbital Navigator. 10, 13, 15–17, 41, 46, 50, 51

PRESTO PRoteus Engineering Simulator for Tests and Operations. 4, 31

PROTEUS Plateforme Reconfigurable pour l’Observation, les Télécommunications Et les Usages Scientifiques. 4–6, 18–21, 25–27, 29–33, 38–41, 43–45, 50, 52, 53, 58

PS Propulsion Subsystem. 55
PSLV Polar Satellite Launch Vehicle. 18

QPSK Quadrature Phase Shift Keying. 26

RAM Random Access Memory. 55, 56
RDP Rate Damping Phase. 33
ROM Read-Only Memory. 55, 56
RSA Reflector Structure Assembly. 14
RWS Reaction Wheels System. 33

SA Solar Array. 4, 44, 45, 48, 51
SADM Solar Array Drive Mechanism. 31, 45, 47, 48, 55
SHM Safe Hold Mode. 13, 27, 32, 33, 36, 41, 43, 53
SLR Satellite Laser Ranging. 14
SOCC Satellite Operations Control Center. 25
SPP Sun Pointing Phase. 33
SRP Solar Radiation Pressure. 19, 20, 34–36
SSA Solid State Amplifier. 29
SSM Secondary Surface Mirrors. 3, 4, 31, 38–40, 51
STA Star Tracker Array. 31, 38, 40, 51
STAM Star Acquisition Mode. 32, 33
STR Star Tracker. 31–33

T2L2 Time Transfer by Laser Link. 13, 14, 41, 46
TC Telecommand Data. 25, 27, 29
TCS Thermal Control System. 4, 6, 38, 40, 41, 46, 55
THU Thrusters. 33
TM Telemetry Data. 25, 27, 29
TOPEX Topography Experiment. 10, 16, 17
TRL Technological Readiness Level. 20, 22
TRSR-2 Turbo Rogue Space Receiver-2. 13, 14, 25
TTC Tracking, Telemetry and Command. 28
TTCM Telemetry Tracking Commanding and Monitoring. 46
TTMTC Tracking Telemetry & Telecommand. 2, 25, 27–29, 55

VAFB Vandenberg Air Force Base. 18

WISE Wide-field Infrared Survey Explorer. 18
WMO World Meteorological Organization. 13

Assignment 1

System Overview & Mission Analysis

1.1 Mission Overview

The Ocean Surface Topography Mission (OSTM), more precisely the JASON-2 satellite, is an international satellite mission that planned to carry on the precise sea surface height measurements initiated in 1992 by the joint mission composed by NASA and CNES: the TOPEX-POSEIDON and continued in 2001 by the NASA/CNES Jason-1 mission.

Researchers wanted to monitor changes in the global sea level and gain a better understanding of the relationship between climate change and the circulation of the oceans through the use of information collected by the mission. This data has been helpful in many fields, such as operational oceanography, seasonal forecasting, climate monitoring, marine meteorology, and research on oceans, the Earth system, and climate. The mission functioned as a link for transferring future measurement collection to international weather and climate forecasting organisations. This information has been used by such organisations to forecast weather and climate across short, seasonal, and long time periods.

The OSTM/JASON-2 took up the previous spacecraft's near-circular orbit at a height of 1336 kilometres (830 miles) above the equator, using the same ground track as Jason-1. It has a period of 112 minutes and a repeating ground track every ten days. Thanks to its inclination of 66° , it was able to provide ocean topography data for 95 percent of Earth's ice-free waters. [52]

1.2 Mission Main Goals

The main high level goal of OSTM/JASON-2 is the continuance of the missions Jason-1 and TOPEX-POSEIDON. In more detail, high level goals of OSTM/JASON-2 can be divided in two main categories as shown in Table 1.1.

Science Goals	Engineering Goals
Continue ocean surface topography measurements	Reach and maintain the same orbit of Jason-1
Investigate ocean circulations	Improve Jason-1 measurement accuracy
Measure global sea level change and its relation to climate change	Maintain stability of measurements accuracy
Improve ocean, coastal tides models and waves measurements	Operate for a minimum period of 3 years

Table 1.1: Science and Engineering goals [52]

1.3 Mission Drivers

Through our analysis of the mission we have identified two drivers:

1. **Continuity with Jason-1 Data.** This is the main driver of the mission. This driver influences the design of most subsystems and the selection of the instruments, as the data accuracy shall be the same

or better with respect to the previous mission and the number of sensors shall remain at least the same.

2. **Accurate Nadir Pointing.** This driver influences the design of many subsystems: the Attitude Dynamics and Control Subsystem (ADCS); the sensor types and positioning on the satellite; the power supply, as the solar panels shall provide a certain minimum amount of power at all times. It is noted that this driver may be considered a consequence of the first, but this driver is also due to the improved measurements accuracy goal of which the first driver is not a consequence.

1.4 Functional Analysis

Starting from the requirements, it is possible to outline the functions necessary for the completion of the mission, as shown in Figure 1.1.

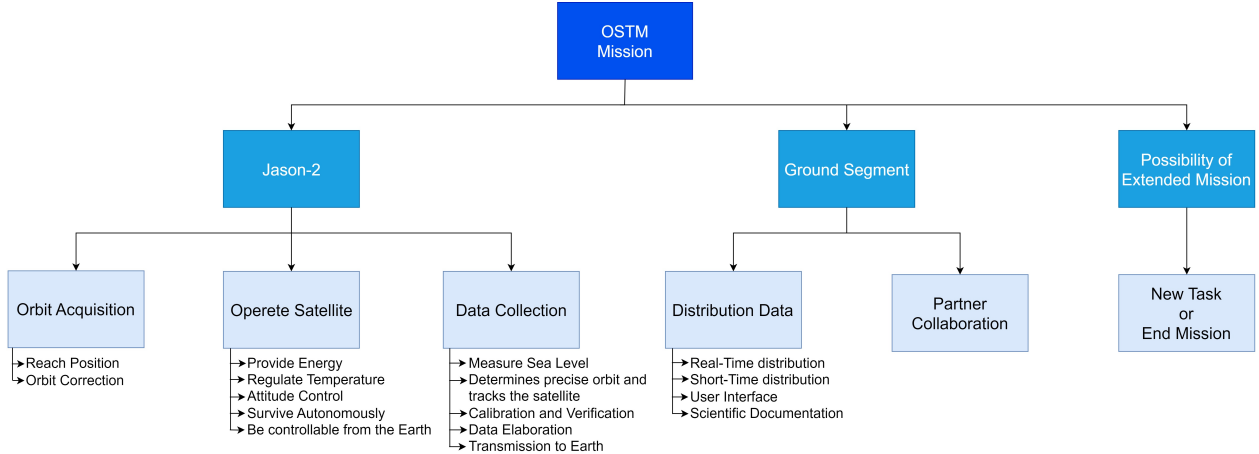


Fig. 1.1: Functional Tree Analysis

1.5 Mission Phases & ConOps

NASA's Press Kit before the launch [52] of the OSTM/JASON-2 mission outlines 6 main phases, which define distinct stages of the mission, each serving a specific purpose:

1. **Launch and Early Orbit Phase (3 days):** This phase involves the launch of the satellite and its maneuvering into its initial orbit. During this time, satellite and instrument systems are activated and thoroughly checked.
2. **Orbit Acquisition Phase (about 1 month):** In this phase, the satellite is maneuvered into its operational orbit. This phase overlaps with the first half of the Assessment Phase.
3. **Assessment Phase (2 months):** This phase begins after the Launch and Early Orbit Phase and concludes when the satellite and instrument systems are certified to be fully functional. It also marks the readiness of the ground system for routine operations.
4. **Verification Phase (at least 6 months):** Overlapping with the Assessment Phase, this phase starts when Jason-2 reaches its operational orbit and flies in tandem with Jason-1. It continues until the received data from the satellite, its instruments, and data processing algorithms are satisfactorily calibrated and validated. During this phase ground data and laser ranging data are collected for verification purposes, furthermore workshops between agencies are held to assess and authorize the delivery of products to final users.
5. **Initial Routine Operations Phase:** Starting after the Assessment Phase and ending three years after launch, this phase involves the continuous collection and monitoring of instrument data. Science data products from the Verification Phase are reprocessed at the end of this phase.
6. **Extended Routine Operations Phase:** If useful data is still being collected, this phase extends the mission by an additional two years or as agreed upon by mission partners.

Within each phase, workshops among partners and reports are also scheduled.

In Figure 1.2, we summarise the main phases inside a broader context containing the Jason-1 and Jason-3 missions as well.

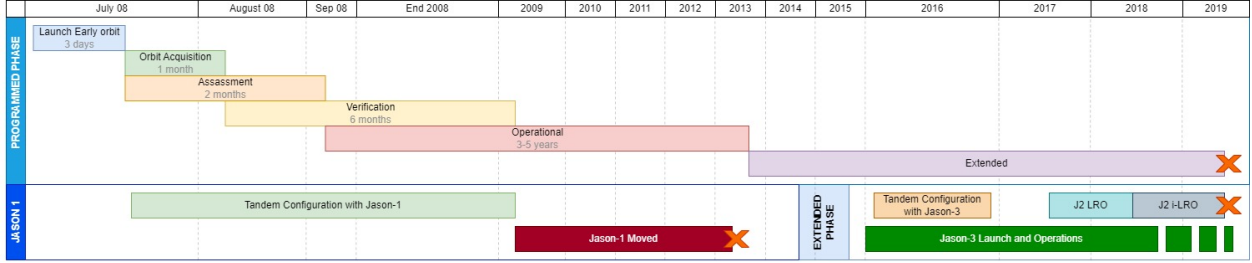


Fig. 1.2: Mission Phase & ConOps

1.5.1 Launch Sequence

The satellite was launched on June 20th, 2008, by a Delta-2 Rocket from the Vandenberg launch site in California, USA. Jason-2's launch timing was meticulously planned to meet its scientific goals, ensuring that the satellite is placed in the correct orbit relatively to the Jason-1 satellite. The launch date was determined by satellite readiness, Delta vehicle availability, and atmospheric conditions at Vandenberg Air Force Base. The launch window was set from June 15th to August 15th, with a nine-minute slot each day, which is brought forward everyday by about 12 minutes. The launch sequence can be summarised in Figure 1.3, which was released by NASA in their pre-launch press kit[52].

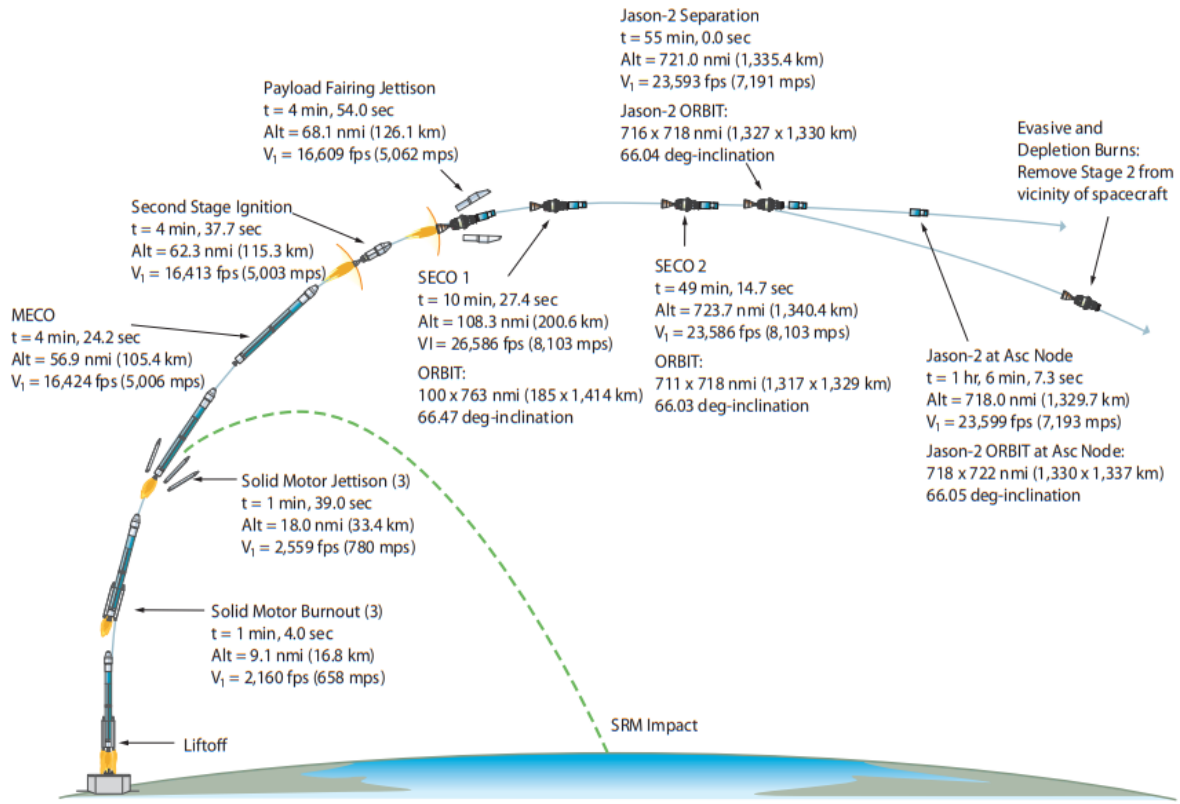


Fig. 1.3: Jason-2 Official Launch Sequence

1.5.2 Extended Phase

The satellite was initially planned to last for 3 to 5 years. However, given the successful outcomes of the Jason-1 mission and the actual lifetime of the Jason-2 satellite, the mission was extended further than the initial estimated lifespan. In the pre-launch documentation [52] the possibility of an "extended mission" is

briefly mentioned.

In this section, we will discuss the end-of-life scenario for the Jason-2 mission, referring to the historical report [8] and the executive report [37] of the mission. The satellite's end-of-life plan closely followed the approach used for its predecessor, Jason-1 [7], ensuring a smooth transition between missions. Jason-2 would operate on its reference orbit until the launch of its successor, Jason-3 [9]. This involved an initial tandem configuration for calibrating and verifying the successor satellite's strumentation, followed by a transition to other orbits. However, there was also the possibility of cancelling the JASON program and terminating the mission. The program's confirmation occurred with the launch of Jason-3 on January 17th, 2016. Following the pattern set by the Jason-1 mission, Jason-2 was then moved to an interleaved orbit at the same altitude in October 2016.

However, due to multiple gyro anomalies and the occurrence of the Safe Hold Mode (SHM), Jason-2 was subsequently moved to a Long Repeat Orbit (LRO) with an 8 km resolution grid in July 2017. This orbit is approximately 27 km below the previous orbit, still utilized by Jason-3. On July 16th, 2018, Jason-2 was relocated to a new Interleaved Long Repeat Orbit (iLRO) to achieve 4 km grid measurements. This increased measurement density was chosen for its advantages in marine geodesy, such as the enhancement of bathymetry and mean sea surface models. On October 1st, 2019, The Jason-2 concluded its science mission after detecting deterioration in the spacecraft's power system [8].

1.6 Scientific Instruments

1.6.1 Overview

In order to accomplish the mission goal, a total of five primary science instruments were carried on board. Three of them are attitude determination systems, to accurately estimate the satellite and position, while the other two were used for sea surface topography measurements. Moreover, three more instruments were carried on board of the spacecraft with their own objectives to fulfill. The data presented in the following section was retrieved from the WMO's OSCAR Website [65] and Dr. Kramer's eoPortal [8]. A brief overview of the scientific instrumentation of the Jason-2 satellite is presented in Table 1.2.

Name	Mass	Power Consumption	Developer
POSEIDON-3	70 kg	78 W	Thales Alenia Space
AMR	27 kg	31 W	JPL/ ATK Space Systems
DORIS	91 kg	42 W	CNES/Thomson
GPSP/TRSR-2	10 kg	17.5 W	Spectrum Astro Inc.
LRA	2.2 kg	-	ITE Inc.
CARMEN-2	4.2 kg	10 W	CNES
LPT	7 kg	15 W	JAXA
T2L2	12 kg	48 W	CNES

Table 1.2: Instrumentation Overview

1.6.2 Payload Description

- **POSEIDON-3**

Positioning,Ocean,Solid Earth, Ice Dynamics, Orbital Navigator (POSEIDON), is a radar altimeter and the main instrument onboard of the spacecraft. Its principal function is measuring the satellite's distance from Earth's surface by emitting radio waves at two different frequencies, 13.575 and 5.3 GHz, towards the sea and measuring the time delay between the return of a signal and the other. Additionally to its main function, POSEIDON-3 can be used to calculate ocean surface current velocity and to measure ocean wave height and wind speed.

POSEIDON-3 features an experimental mode to support measurements closer to coastal zones. This will be achieved by an open loop tracker as the satellite to surface distance will be estimated by the altimeter using the real-time orbit position predicted by DIODE (on board navigator based on DORIS receiver).

- **DORIS**

Doppler Orbitography and Radiopositioning Integrated by Satellite (DORIS) is a Precise Orbit Determination (POD) system providing position and ionospheric correction for POSEIDON-2. The DORIS

flight segment consists of a two-channel, two-frequency (401.25 MHz and 2036.25 MHz) Doppler receiver capable of tracking signals from a worldwide network of about 50 ground beacons.

- **AMR**

The Advanced Microwave Radiometer (AMR) is a JPL-developed instrument, which derives from its predecessor: the Jason Microwave Radiometer (JMR), positioned on the Jason-1 satellite. The AMR is divided in two subsystems: the Electronics Structure Assembly (ESA) and the Reflector Structure Assembly (RSA).

The AMR is a passive microwave radiometer measuring the brightness temperatures in the nadir column at frequencies of 18.7, 23.8, and 34 GHz, providing path delay correction for the altimeter. The 23.8 GHz channel is the primary water vapor sensor, the 34 GHz channel provides a correction for non-raining clouds, and the 18.7 GHz channel provides the correction for effects of wind-induced enhancements in the sea surface background emission.

- **GPSP/TRSR-2**

The Global Positioning System Payload (GPSP), which is also referred to as Turbo Rogue Space Receiver-2 (TRSR-2), is a 16-channel GPS receiver with the objective to provide supplementary positioning data to DORIS in support of the POD function.

The GPSP is fully redundant and divided in two independent receivers operating in cold redundancy. Each unit is composed of an omnidirectional antenna, a low-noise amplifier, a crystal oscillator, sampling down-converter, and a baseband digital processor assembly.

- **LRA**

The Laser Retroreflector Array (LRA), provides a reference target for Satellite Laser Ranging (SLR) measurements, which are necessary to calibrate the POD system and the altimeter throughout the mission. The LRA is a totally passive unit placed on the nadir face of the satellite and is composed by nine quartz corner cubes arrayed as a truncated cone with one in the center and the other eight distributed around the cone. The small number of ground stations and the sensitivity of laser beams to weather conditions make it impossible to track the satellite continuously using only this instrument, for this reason other onboard location systems are needed.

- **CARMEN-2**

The Environment Characterization and Modelisation 2 (CARMEN-2) is an instrumentation dedicated to study the influence of space radiation on advanced components to measure high-energy particle flux of electrons (e^-) and protons (p^+), and ion fluxes.

The instrument is composed of a spectrometer and an Experiment Module (MEX). The MEX includes three types of dosimeters to measure accurately the exposed dose and monitor several components under test.

- **T2L2**

The main function of the Time Transfer by Laser Link (T2L2) instrument is to allow comparison and follow-up of distant clocks, either of an embarked clock relative to a ground clock or of two (or more) ground clocks. The means used to establish a link between these clocks is the transmission and the dating of laser pulses.

The T2L2 satellite payload is composed of two subsystems:

- * The optical subsystem that ensures the functions of electronic activation and collection of the laser pulse for the dating.
- * The electronic subsystem that ensures the functions of non-linear detection, dating, instrument management and interfacing with the satellite.

- **LPT**

The Light Particle Telescope (LPT) is a detection unit developed by JAXA. LPT is composed by two units:

- * LPT-E provides functions of the electrical interface with the satellite system. It receives primary power supply from the satellite system and provides sensors and electrical circuits with secondary power. It also receives prompts and sends telemetry data to the ground segment.
- * LPT-S consists of four sensors. Each sensor counts a number of interesting particles irradiated from inside of the view angle with the specific energy of each channel every second.

Figure Figure 1.4 shows the position of the payloads on the spacecraft.



Fig. 1.4: Payloads on board of Jason-2

1.6.3 Main Goals - P/L correlations

Mission Goal	Payload
Measurement of sea level	POSEIDON-3
Precise orbit determination and tracking the satellite	DORIS, GPSP, LRA

Table 1.3: Correlation between mission main goals and payloads

1.6.4 ConOps - P/L correlations

Mission phase	Payload
Launch and Early Orbit Phase	Activation of positioning systems DORIS, GPSP, LRA
Orbit Acquisition Phase	DORIS, GPSP, LRA
Assessment Phase	Testing and calibration of POSEIDON-3 and AMR
Initial Routine Operations Phase	Employement and manteinance of all scientific payloads
Extended Operations Phase	-

Table 1.4: Correlation between mission phases and payloads

1.7 Mission Analysis

1.7.1 Nominal Orbit

Jason-2's nominal orbit is identical to that of Jason-1, its high altitude (1336 kilometers) reduces interactions with the Earth's atmosphere and gravity field to a minimum, thus making orbit determination easier and more precise. The orbit inclination of 66 degrees enables the satellite to cover most of the globe's unfrozen oceans. The orbit's repeat cycle is just under 10 days. This cycle is a trade-off between spatial and temporal resolution designed for the study of large-scale ocean variability.

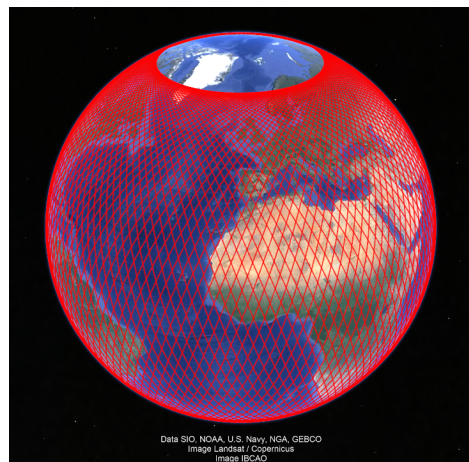


Fig. 1.5: 3D Ground Track for a 10-day cycle [3]

Furthermore, using the same orbit as TOPEX-POSEIDON will ensure better intercalibration and data continuity. The orbit is also designed to pass over two dedicated ground calibration sites : Cap Senetosa in Corsica and the Harvest oil rig platform in California, USA.

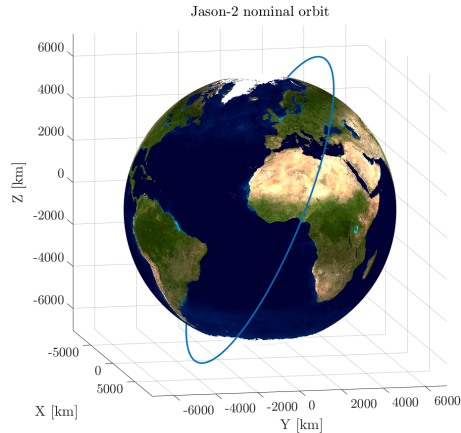


Fig. 1.6: Single Orbit Plot

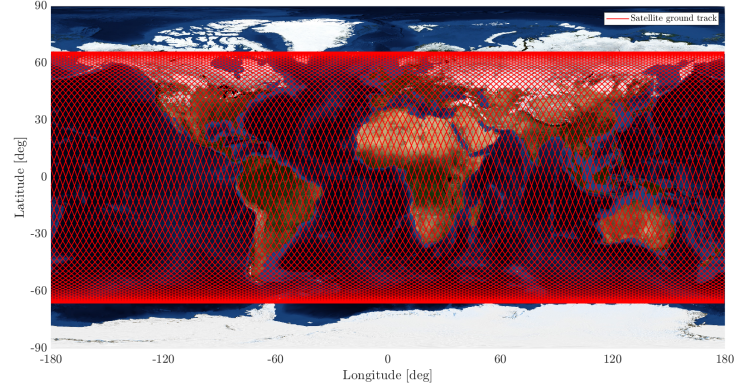


Fig. 1.7: 2D Ground Track for a 10 day cycle

1.7.2 Orbits History & Phase Correlation

After launch, the satellite finds itself in a parking orbit, from which it is moved to the nominal orbit thanks to the propulsive system on board, during the "Orbit Acquisition Phase". During the first six months of the mission, period known as the "Verification Phase", the OSTM/JASON-2 and Jason-1 satellites were flying in formation along the same groundtrack, separated in time by only 55 seconds. This tandem configuration allows in-depth intercalibration of the two altimeter missions. During "Verification" and "Operational" phases Jason-2 was located on its nominal orbit.

From Oct.2016, after more than 8 years of service, Jason-2 shifted to the interleaved orbit that was used by TOPEX-POSEIDON from 2002-2005 and Jason-1 from 2009-2012. This interleaved orbit has a groundtrack in-between the nominal groundtrack. The Jason-3 satellite continued the long term climate data record on the nominal ground track.

From July 2017, Jason-2 operates on a new Long Repeat Orbit (LRO) at roughly 1309.5 km altitude.

From July 2018, Jason-2 operates on an Interleaved Long Repeat Orbit (iLRO), with a ground track in the middle of the grid defined by the LRO. (More details in subsection 1.5.2)

The satellite decommissioning operations were completed on the 10th of October, 2019, and deorbiting is expected to happen throughout hundreds of years due to passive atmospheric drag.

1.7.3 Orbit maintenance

A satellite's orbit parameters tend to change over time as a result of atmospheric drag. In the long term, more or less periodic variations also occur due to instabilities in the Earth's gravity field, solar radiation pressure, and other forces of smaller magnitude.

Orbit manoeuvres are performed every 40 to 200 days. Intervals between maneuvers depend mainly on solar flux and each maneuver lasts 20 to 60 minutes. Where possible, they are performed at the end of the orbit cycle and above solid earth, so that lost data acquisition time is reduced to a minimum.

Assignment 2

Mission Analysis & Propulsion Subsystem

2.1 Mission Analysis

The OSTM/Jason-2 satellite lies on the same orbit as Jason-1 and the original TOPEX/POSEIDON mission. This creates a 10-day repeating ground track, in which 127 revolutions are completed during each cycle.

The mean classical orbit elements and other auxiliary data are given in Table 2.1 and Table 2.2 [38].

Orbit element	Value
Semi-major axis	7741.43 km
Eccentricity	0.0000095
Inclination	66.04 deg
RAAN	116.56 deg
Argument of periapsis	90.0 deg

Table 2.1: Mean classical orbit elements

Auxiliary Data	Value
Nodal Period	112,4285 min
Repeat Period	9.9156 days
Number of revolutions within a cycle	127
Equatorial cross-track separation	315 km
Orbital speed	7.2 km/s
Ground track speed	5.8 km/s

Table 2.2: Auxiliary Data

2.1.1 Orbit Choice

In order to guarantee consistency with objectives and preserve programme continuity, it was decided that the mission had to continue on the same orbit as Jason-1. The most crucial aspect of the orbit is its inclination of 66° , chosen in order to cover most of the globe's unfrozen oceans, as depicted in Figure 2.1. The orbit is nearly circular to optimize resolution and observability. Its high altitude of 1336 km reduces interactions with the Earth's atmosphere and gravity field to a minimum, thereby facilitating more precise orbit determination and easier station keeping. Additionally, the orbit is designed to pass over two dedicated ground calibration sites: Cap Senetosa in Corsica and the Harvest oil rig platform in California, USA. [38]

2.1.2 ΔV Estimation

In the forthcoming analysis, we aim to quantify the ΔV necessary for the mission's entirety. We operate under the assumption that the mission primarily focuses on orbit maintenance, thereby omitting considerations for end-of-life phases. We do not include the manoeuvres to transition between orbits (LRO and iLRO) in our analysis as they are not pre-programmed but rather regarded as possibilities, akin to the situation observed in the Jason-1 mission.

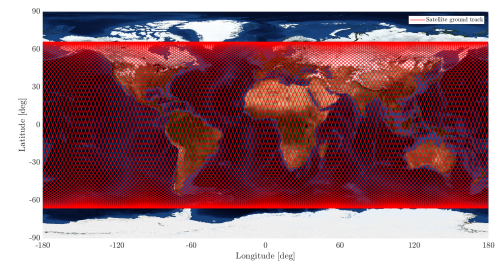


Fig. 2.1: 2D Ground Track for a 10 day cycle

To reach the desired orbit for the mission and calculate the total ΔV needed to achieve the agreed upon goal, the mission is divided into distinct phases, each of which has its own criticalities and solutions.

2.1.3 Launcher Selection

According to the PROTEUS documentation [26], the mounting system for Jason-2 is compatible with various launch vehicles, including Ariane V, Delta II, PSLV, Rockot, Soyuz, Taurus, and many other. To determine the most suitable option for our specific orbit, several factors need to be considered. The primary constraint for launcher selection is the 66° inclination, which varies depending on the launch site. As depicted in Figure 2.2, our options are limited to the Vandenberg Air Force Base (VAFB), Kourou (Guiana Space Centre), and Russian or Indian launch sites.

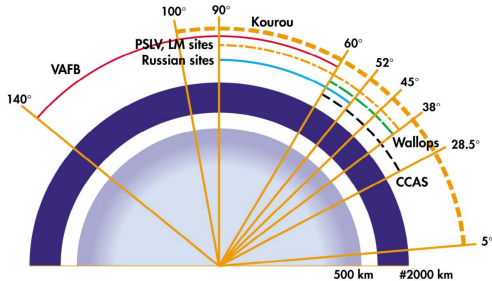


Fig. 2.2: Achievable orbits vs launch sites and vehicles

Next, the fairing volume compatibility is evaluated, setting the minimum diameter at 1.910 m and a height of at least 2.218 m, excluding the nose cone. This is constrained by the PROTEUS platform dimensions of $1.910 \times 0.954 \times 1$ m and the Jason-2 payload dimensions of $0.954 \times 0.954 \times 1.218$ m.

Finally, the ΔV that each launcher can provide is controlled to make sure it respects the missions minimum requirements. A rough estimate is performed starting from the ideal velocity equation $\Delta V_{\text{ideal}} = \sqrt{\frac{\mu}{R_0}} \sqrt{2 - \frac{R_0}{R_0 + h}}$ [48] and the Earth's rotation contribution $\Delta V_{\text{rot}} = V_E \cos(i)$ [48]. Losses are then incorporated in the equation, this is done considering worst-case scenarios for gravity (1.3 km/s) and drag (0.15 km/s) as explained in the Wertz, Everett, Puschell book [64] and implementing the ESA margin guideline of 2% [24]. From this estimate a required ΔV of approximately 10 km/s is obtained.

Launchers	Success	Launch site	Usable volumediameter [mm]	ΔV compatible	\approx Cost [\$ milion]
Ariane 5	100 % (23/23)	Europe/Kourou	4570 or 4800	Oversized [46]	150
Delta 2 7320-10	98 % (163/165)	CCAFS or VAFB	2743	v7320-10: Compatible [59] v7920 and more: Oversized	51-137
PSLV	94 % (17/18)	India/Shriarikota	2900	Not found	30
Rockot	94 % (16/17)	Russia	2520	Compatible [45]	41.8
Soyuz	94 % (1654/1753)	Russia	3395	Oversized [56]	80
Taurus	75 % (6/8)	CCAFS or VAFB	2055	v2210: Little Margin v2110: Compatible [54]	40-50

Table 2.3: Launcher Data until 2011

For this mission, the selected launcher was the Delta 2-7320-10C, featuring a dual-stage configuration and a 10-foot fairing height (3 meters), enough to accommodate the Jason-2 satellite. While our analysis also considered Rockot and Taurus as viable, cost-effective alternatives; the high success rate and extensive track record of the Delta 2, on top of the continuity with the Jason-1 mission (which was also launched utilizing Delta 2) probably led to its selection by Jason-2's team.

2.1.4 Orbit Acquisition

Taking into account the selection of the Delta 2 launcher, its manual documents[59] declare an injection precision of ± 9.3 km on perigee altitude and ± 0.05 degrees on inclination (with a 3σ dispersion). In a similar mission named WISE, the maximum error in mean anomaly is estimated to be within ± 7.5 minutes [60]. Considering the worst-case scenario, the ΔV can be estimated using a plane change followed by a shape change and a phasing maneuver of the duration of more or less 70h to rendezvous behind Jason-1.

In this way, a total $\Delta V = 13.4\text{m/s}$ is obtained, to which a 5% margin has to be added according to the ESA margin guidelines [24]. So the final requirement for this phase is $\Delta V = 14.07\text{m/s}$, which corresponds to $\Delta m = 3.28\text{kg}$ of hydrazine used.

This value is a gross estimate and may not accurately reflect reality. During the Jason-2's orbit acquisition, outlined in Figure 2.3, orbit corrections and testing persisted for 20 days, which resulted in the consumption of 3.5 kg of hydrazine through three main maneuvers utilizing four thrusters each (OCM4), with a magnitude of approximately 3 m/s for each maneuver, alongside other maneuvers of lesser significance [44].

2.1.5 Station Keeping

A satellite orbit slowly decays over time due to air drag, Earth's non-homogeneous gravity field, Solar Radiation Pressure (SRP), and smaller perturbations. Periodic maneuvers are required to keep the satellite in its nominal orbit. Each orbit maintenance maneuver is performed using only two thrusters (OCM2) to minimize the amount of fuel consumed.

In the 2009 mission overview [43] it is outlined how the station keeping maneuvers are performed approximately once every 2 months in order to keep the satellite inside a $\pm 1\text{ km}$ range from its nominal altitude. By considering a simple Hohmann transfer between the nominal orbit and the extremities of this range, and applying this maneuver once every 2 months; the total yearly ΔV is 2.78 m/s ($\Delta m = 0.625\text{kg}$). To this value a twofold margin has to be applied, as per ESA Guidelines [24], which brings the total yearly ΔV to 5.56 m/s , or about 1.29 kg of fuel consumed every year.

2.1.6 Margins and Comparison

Launcher Selected	$\Delta V [\text{m/s}]$			Mass [Kg]		
	Reverse Engineering			True Data	Reverse Engineering	True Data
	Calculated	Margin	Total			
Orbit Acquisition	13.4	5 %	14.7	15.01	3.28	3.5
Station Keeping	2.78 (for year)	100 %	61.18 (for 11 years)	23.80	14.20	(estimated $\approx 0.5\text{ kg/year}$)
Interleaved LRO i-LRO	not considered		0	11.91	not considered	2.73
Fuel Depletion			0	2.41		(estimated - not found)
END			0	50.16		0.55
	4 kg (for emergency)		18.02	19.82		11.32
	Total	93.27 m/s	123.11 m/s	21.48 Kg	25.27 Kg	4.4
						0

Table 2.4: Mass and Velocity Comparison

As highlighted in Table 2.4, the actual station keeping costs were much lower than what was expected at the beginning of the mission, this left room for other maneuvers once the initial mission of the satellite was ended, such as the movement on the LRO and successively on the iLRO. Another aspect which wasn't initially considered is the remainance of fuel once the satellite was set to be decommissioned, this was solved by depleting most of the fuel left, keeping a small quantity for emergencies. This small remainance is kept for any emergency maneuver needed, such as avoiding any collision with active satellites, and amounted to approximately 4 kg of hydrazine. All of the real data of the satellite was taken from the 2018 Mission Status Report from the CNES [33].

2.2 Propulsion System

2.2.1 Propulsion System Overview

The Jason-2 propulsion system is part of the Plateforme Reconfigurable pour l'Observation, les Télécommunications Et les Usages Scientifiques (PROTEUS). PROTEUS is a 3-axis stabilized platform designed for satellite missions in Low Earth Orbit (LEO) and has a mass of 265kg [25]; it includes the solar panels, attitude control systems, propulsion systems, data storage, and telecommunication systems for the satellite it services. The

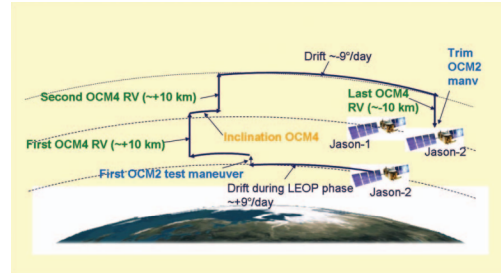


Fig. 2.3: Orbital acquisition strategy

PROTEUS platform was used for all Jason-1, Jason-2 and Jason-3 missions.

The propulsive system of PROTEUS is a monopropellant system, which means that the energy source is chemical and stored in a single compound, hydrazine in this case. Specifically PROTEUS's propulsion system is a pressure-fed blowdown system, in which the pressurising gas, Nitrogen N₂, is stored in the same tank as the propellant from which is divided through a diaphragm. The system is composed of four 1N thrusters, which decompose the hydrazine through a catalyst. The chemical energy in the hydrazine bonds is transformed in enthalpy, through the decomposition reaction with the catalyst, and then in kinetic energy through the nozzle.

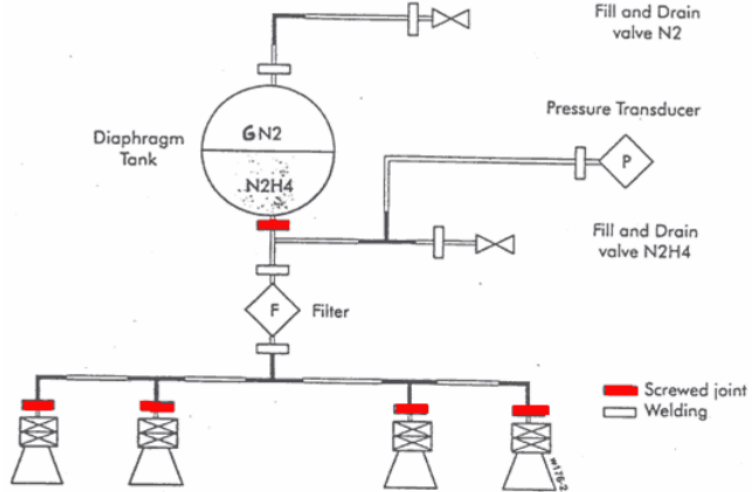


Fig. 2.4: Schematic of PROTEUS's Propulsion System

The PROTEUS propulsion system has to provide a ΔV for three main functions:

- **Orbit Injection Correction:** the launcher injects Jason-2 in a Launch and Early Orbit Phase (LEOP) 10 km below the nominal orbit with all other orbital parameters as close to nominal as possible. The propulsion system shall provide the ΔV needed to correct any deviated orbital parameters.
- **Station Keeping:** due to SRP, air drag, and J2 perturbances the orbital parameters deviate in time. The propulsion system shall provide the ΔV needed to keep the spacecraft on the nominal orbit.
- **End of Life Maneuvers:** the propulsion system shall provide the ΔV needed to perform any extra maneuvers at the end of its mission life, such as making room on the orbit for its successor or deorbiting the satellite.

Due to the nature of these requirements the propulsion system in this case can be categorized as a ***secondary*** propulsion system, even if it is the only one present on the satellite, due to the low ΔV it has to provide. The ***primary*** propulsion system is technically the launcher itself, which provides all the ΔV needed for injection (roughly three orders of magnitude larger).

2.3 Propulsion System Sizing and Analysis

Due to its very high Technological Readiness Level (TRL) and its successful implementation in the Jason-1 mission, a hydrazine monopropellant blowdown propulsion system was selected for the Jason-2 mission. This system configuration has been used extensively in the past and has proven to be economical, versatile, and reliable.

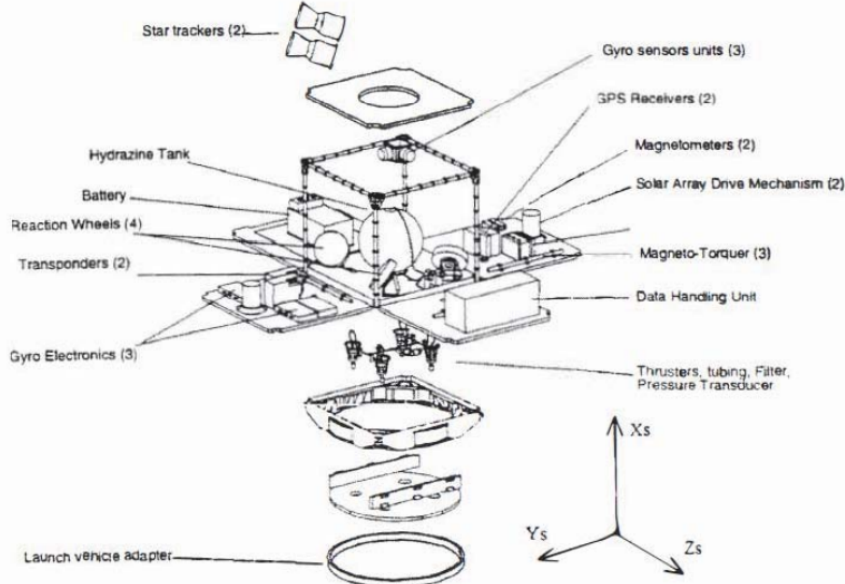


Fig. 2.5: PROTEUS internal view [11]

The sizing present in the following sections is based on the thrusters data [1] used on the PROTEUS platform. The constants used in the following sections are: $g_0 = 9,80665 \text{ m/s}^2$, $R_{N2} = 296,8 \text{ J/kgK}$.

2.3.1 Propellant Selection and Masses

Hydrazine was specifically selected because of its stability, high performance in the form of specific impulse and clean exhaust.

The dry mass $m_{dry} = 477 \text{ kg}$ is obtained from the subtraction of the launch mass of 505 kg [25] and the true propellant mass of 28 kg [25]. Considering the obtained m_{dry} , the ΔV requirement of 123 m/s (calculated from launch and propellant masses [25] through the Tsiolkovsky rocket equation) and considering that the thrusters have a $I_{SP} = 220 \text{ s}$, the required fuel load m_f can be calculated using the Tsiolkovsky rocket equation:

$$\Delta V = I_{SP} \cdot g_0 \cdot \ln \left(\frac{m_{dry} + m_{prop}}{m_{dry}} \right) \quad (2.1)$$

$$m_{prop} = 1.03 \cdot 1.02 \cdot 1.005 \cdot m_{dry} \cdot \left(e^{\Delta V / I_{SP} \cdot g_0} - 1 \right) \quad (2.2)$$

An ullage of 3% is considered along with residuals of 2% (MAR-MAS-080) and an extra 0.5% for loading uncertainties. The required fuel load is then $m_{prop} = 29,55 \text{ kg}$.

2.3.2 Tank Sizing and Masses

A blowdown titanium spherical tank is implemented for the mission. The tank is equipped with a diaphragm made from EPN-40 (EPDM type silica-free rubber [16]), as it's compatible with hydrazine's corrosiveness and has a high specific strength. Nitrogen is used as pressurant due to the fact that it's less prone to leakage with respect to Helium and because it's relatively cheap.

To calculate the required tank volume and pressurant mass, the ideal gas model is assumed and the propellant is assumed to be kept at a constant temperature of $T_{tank} = 298 \text{ K}$ [32]. At the given temperature, hydrazine has a density of $\rho_{prop} = 1003,6 \text{ kg/m}^3$ [53] and as such the total volume of hydrazine is $V_{prop} = 29,44 \text{ L}$.

The thruster has an inlet pressure range of $22 \text{ bar} - 5,5 \text{ bar}$, considering feed losses of $\Delta P_{feed} = 0,5 \text{ bar}$, the tank pressure range should be between $P_i = 22,5 \text{ bar}$ and $P_f = 6 \text{ bar}$. This produces a blow down ratio of $B = 3,75$. The volume of gas can be calculated with the following formula assuming isothermal flow and taking into account an extra 10% margin of unused propellant volume (MAS-CP-010).

$$V_{gas,i} = V_{prop} \left(\frac{1}{B - 1} + 0.1 \right)$$

The obtained value is $V_{gas,i} = 13,65L$.

The mass of pressurant can be calculated, including a 20% margin, using the following formula:

$$m_{gas} = 1.2 \cdot \frac{P_i \cdot V_{gas,i}}{R_{N2} \cdot T_{tank}}$$

An $m_{gas} = 0,417kg$ is obtained.

The required tank volume can be calculated, taking into account an extra 1% extra volume taken by the balder, with: $V_{tank} = 1.01(V_{gas,i} + V_{prop})$. And $V_{tank} = 43,52L$ is obtained. The radius of the tank is $r_{tank} = 218,2mm$.

The properties of Ti-6Al-4V are: $\rho_{tank} = 4430kg/m^3$ and $\sigma = 1100MPa$ [22]. Assuming a thin wall approximation, the required thickness of the tank walls can be calculated with the following formula:

$$t_{tank} = \frac{f_s \cdot P_i \cdot r_{tank}}{2\sigma}$$

Considering a safety factor of $f_s = 2$, a value of $t_{tank} = 0,446mm$ is obtained.

The final external diameter of the tank is $d_{tank} = 437,3mm$. Finally the mass of the tank can be obtained through the formula:

$$m_{tank} = \rho_{tank} \cdot \frac{4}{3}\pi \cdot \left((r_{tank} + t_{tank})^3 - r_{tank}^3 \right)$$

Which gives a mass of $m_{tank} = 1,185kg$.

The values obtained are compared to the actual mission data in Table 2.5

	Calculated	Actual
m_{prop}	29,55kg	28kg
V_{tank}	43,52L	37,5L
d_{tank}	437,3mm	420mm
m_{tank}	1,185kg	3,9kg

Table 2.5: Comparison between the calculated data and the actual data [16]

2.3.3 Feeding Lines

As visible in Figure 2.5, the feeding lines of the system are in an "H" configuration connected in the middle to the tank and at the vertices to the four thrusters. This allows for a compact, economical and not so complex configuration, considering the absence of valves and redundancies in the lines. This absence can be justified by the fact that the system is classified as a secondary propulsion system and that the system's TRL is very high.

Along the feeding lines a pressure transducer is placed, this is useful for knowing the amount of propellant at any given time in the tanks. Indeed knowing the tank volume $V_{tank} = 37,5L$, the temperature $T_{tank} = 298K$ [32], the density of the propellant $\rho_{prop} = 1003.6kg/m^3$ [53] and the measured pressure P_m :

$$V_{gas} = \frac{m_{N2} \cdot R_{N2} \cdot T_{tank}}{P_m}$$

Having the current N2 volume, the propellant volume can be calculated:

$$V_{prop} = V_{tank} - V_{gas}$$

From which the mass of propellant is obtained:

$$m_{prop} = \rho_{prop} \cdot V_{prop}$$

At last, knowing the thruster's specific impulse $I_{sp} = 220s$ and dry mass $m_{dry} = 477kg$, the available ΔV can be obtained through the Tsiolkovsky equation (2.1).

2.3.4 Thrusters

This propulsion system makes use of four 1N thrusters placed in a square configuration angled parallelly to the X axis of the satellite, as shown in Figure 2.5. This configuration is convenient as attitude control is not required from the system and firing two thrusters at opposite ends or four thrusters at a time does not change the attitude of the satellite. Since the thrusters are not gimbaled, the satellite has to be rotated by the attitude control system to provide thrust in a specific direction . This configuration has the advantage of having a low complexity and cost, but has as a downside the fact that, while the propulsion system is providing thrust, the satellite can't be in its nominal data-acquisition mode.

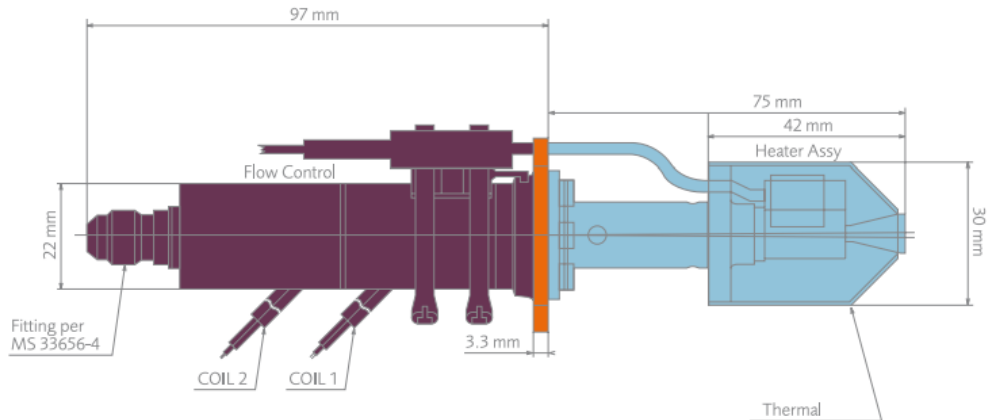


Fig. 2.6: 1N Thrusters schematic [1]

As said before, the thrusters are usable in configurations of two or four at a time respectively as OCM2 and OCM4 modes, this allows for two different thrust options. These thrusters are also not throttled, due to a lack of a valve for flow control in the feeding line. The thrust diminishes in direct correlation to the mass flow of the propellant. The less propellant is in the tank, the lower the pressure is in the system, the lower is the mass flow, due to the blowdown structure of the system.

The thrusters have two independent valves for redundancy, as well as a heater to ease the start up and is designed for both, long term steady state and pulse mode operations [1] .

Assignment 3

Tracking Telemetry & Telecommand Subsystem

Change Long	
§ 3.1.1	pp 25: Rephrase the text and justify the selection of the ground station position
§ 3.1.2	pp 25: Rephrase and remove unclear parts pp 25: Add justification for the antenna position in the configuration pp 25-26: Move the description of Table 3.1 into subsection 3.1.2 pp 26: Remove a image due to page constrains, but linked with Figure 7.5
§ 3.1.3	pp 26: Update to a combination of Reed-Solomon and Convolutional encoding pp 26: Justify the choose Reed-Solomon and Viterbi combination
§ 3.2	pp 26-27: Add a rough estimation of contact windows and data volume transferred
§ 3.2.2	pp 27: Update downlink data-rate following eoPortal data [8]
§ 3.3.1	pp 28: Specify the selection of frequency from Table 3.1 pp 28: Add Table 3.2 with the ground stations information on size, frequency, and losses
§ 3.3.2	pp 28: Table 3.3 is the combination of two old tables to address page constraints
§ 3.3.3	pp 29: Correction of frequency
§ 3.3.4	pp 29: Review some calculations pp 29: Add bandwidth calculation and SNR_{margin} discussion

3.1 Architecture and Design

3.1.1 Ground Segment Architecture

The Tracking Telemetry & Telecommand (TTMTC) subsystem is a vital component of any satellite mission, acting as the nervous system that allows the satellite to communicate with its ground stations. The raw engineering Jason-2 data is recorded onboard and then transmitted to the three "command and telemetry" ground stations. A simplified schematic of the ground segment system architecture is illustrated in Figure 3.1. As detailed in Figure 3.2, the stations for OSTM/Jason-2 are strategically located in Usingen (Frankfurt, Germany), Wallops (Virginia, USA), and Fairbanks (Alaska, USA), maintaining continuity established by the Jason 1 mission to avoid additional building costs. In addition to these Earth terminals, the ground control system includes a satellite control center at CNES and a Satellite Operations Control Center (SOCC) at NOAA in Suitland, Maryland, near Washington, D.C.

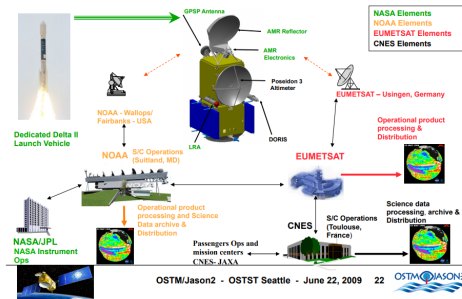


Fig. 3.1: Jason 2 System Architecture

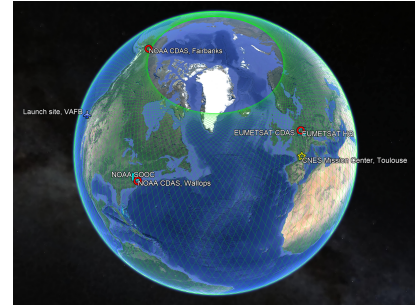


Fig. 3.2: Ground Stations

During launch, satellite tracking ground stations in South Africa, Kiruna (Sweden), and Kourou (French Guiana) will supplement the existing network. The ground station in Hartebeesthoek, South Africa, is responsible for confirming the separation of OSTM/JASON 2 from the Delta II rocket.

To ensure the proper functioning of the satellite, it needs to establish connections with other spacecraft and specialized stations. Specifically, contact with ground stations such as Harvest, California (USA)[30] and Cap Senetosa, Corsica (France)[29] is required for the calibration of the Precise Orbit Determination (POD) system [51], consisting of various components such as DORIS, TRSR-2 (GPSP), and LRA. In particular, DORIS utilizes a ground network of approximately 60 ground beacons.

Finally, to conclude the space segment, the satellite can communicate through a GPS receiver, which maintains an average connection with 8 GPS satellites simultaneously[34].

3.1.2 Signal Elaboration and TTMTC Architecture

In this chapter, will be studied and modelled only the main telemetry and control communication. This task is entrusted to the PROTEUS platform, which communicates with Earth through two spiral-shaped Medium Gain Antennas (MGA) that operate in the microwave S-band. As shown in Figure 7.5, the two antennas are pointing in opposite directions to guarantee data transfer for all possible orientations of the satellite, especially one antenna is oriented towards Earth during a nadir-pointing configuration, while the other serves as a redundancy. According to PROTEUS documentation [26], a Data Handling Unit (DHU) is used by the payload on Jason-2 to interface with the Proteus platform. The DHU is in charge of a number of duties, such as creating, preserving, and downlinking Telemetry Data (TM) as well as elaborating and executing Telecommand Data (TC) that it receives from the ground stations.

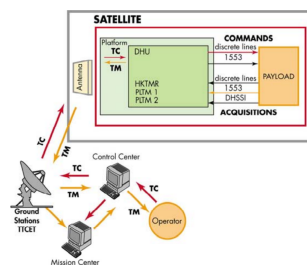


Fig. 3.3: PROTEUS Data Path Scheme

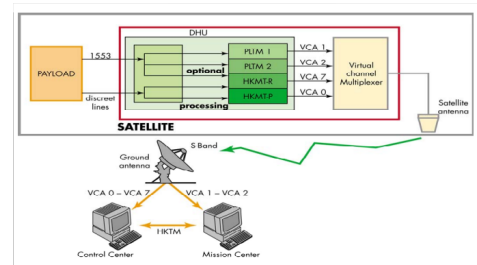


Fig. 3.4: PROTEUS Telemetry Scheme

The overall payload data path is shown in Figure 3.3, while the specific telemetry flow from the payload to the ground system is shown in Figure 3.4.

3.1.3 Signal Selection

The Proteus manual [26] suggests three sets of S-Band frequencies as detailed in Table 3.1. However, the choice is contingent upon the satellite's orbit and the availability of already allocated frequencies, for which precise data is currently unavailable.

	Up-link frequency	Down-link frequency	UIT publication
Couple 1	2040.34300 - 2040.64300 MHz	2214.920 - 2216.920 MHz	AR/11A/1828
Couple 2	2088.72819 - 2089.02819 MHz	2267.515 - 2269.415 MHz	AR/11A/1826
Couple 3	2101.56000 - 2101.86000 MHz	2281.400 - 2283.400 MHz	AR/11A/1827

Table 3.1: Frequency couples reserved at UIT for PROTEUS

The S-band is a particular section of the microwave band that ranges from 2 to 4 GHz. In the recent years it has been devoted to satellite telecommunication, as the S-band offers several advantages for satellite communication. Its signals can penetrate through atmospheric conditions more effectively compared to higher frequency bands, which makes it suitable for reliable and robust communication, particularly in challenging weather conditions or densely populated areas where signal interference may occur.

Since the Jason-2 has to sustain almost real-time communication in every condition, choosing frequencies in the S-class for uplink and downlink should guarantee the reliability needed with the required data rate.

Additionally, Jason 2 use a combination between Reed-Solomon and Viterbi convolutional encoding, with QPSK as modulation. The CCSDS communication protocol standard is also used in the forward and return link mode. [8]

Combining Reed-Solomon coding with Viterbi convolutional encoding is a standard in space communication. Reed-Solomon corrects burst errors, while Viterbi convolutional encoding reduces random errors, creating a robust system that ensures data integrity in noisy environments. [36]

Quadrature Phase Shift Keying (QPSK) is a type of digital modulation scheme that is commonly implemented in satellite communication systems. This has a series of advantages over other modulation schemes, the main ones are:

- **Higher data rates:** QPSK is able to transmit data at a higher rate than other modulation schemes, as it can encode two bits of information per symbol, rather than just one. This makes it suitable for applications that require high data rate such as telemetry transmission.
- **Improved performance in noisy environments:** QPSK is more resistant to noise and interference than other modulation schemes, as it is able to transmit information using both phase and amplitude changes in the carrier signal. This makes it more robust in noisy or fading environments, such as those found in Earth-pointing satellite communications.
- **Greater spectral efficiency:** QPSK requires less bandwidth than other modulation schemes for a given data rate. This makes it more spectrally efficient, which is important in satellite communication systems where bandwidth is a limited resource.

3.2 Modes and Mission Phases

During its lifetime, the Jason-2 satellite's data volume and contact strategy varied depending on numerous factors, such as signal disturbances, sensor or system failure, data type and format for downlink and much more. In this section the initial requirements will be analyzed and subsequently the mission phases telemetry and telecommand are better explained.

Due to the lack of available data, it is important to estimate roughly the durations of contact windows and the volumes of data transferred per pass. Based on simple geometric considerations [12], the satellite remains in contact with ground stations for approximately 12.35 minutes per orbit, assuming communication with at least one ground station. With a real downlink speed of 958.25 kbit/s considering encoding and modulation techniques (see Equation 3.5), this results in 88.72 MB/pass. Since the satellite completes approximately 13

passes daily, with an orbital period of about 112 minutes, the total data transmission amounts to 1.13 GB per day.

3.2.1 Initial Requirements

On the PROTEUS User's Manual [26] some limitations of the PROTEUS's TTMTC subsystem are highlighted:

- The maximum size of the source packet shall not exceed 1 kbyte ($512 \cdot 16$ bits) to prevent data losses and avoid longer transmission periods.
- The uplink data-rate shall be fixed at 4 kbit/s for the whole lifetime of the spacecraft, independently from the active mode of the satellite [8].
- The downlink data-rate during all routine phases shall be 838 kbit/s at maximum [8].
- The downlink data-rate during emergency phases shall be 85.966 kbit/s at maximum [26].

3.2.2 Satellite Active Modes

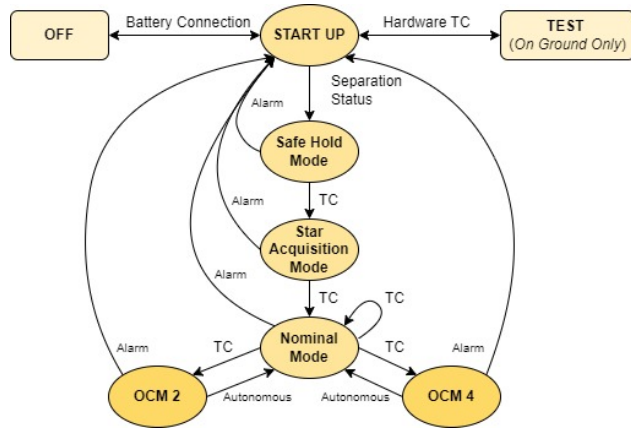


Fig. 3.5: Jason-2's Phases [26]

Telemetry and telecommand strategies vary in function of the current active mode of the satellite. The main active modes are explored in the following paragraph:

- During Launch the satellite receivers are active, making possible issuing Telecommand Data for the satellite to follow.
- While in Nominal Mode the satellite operates maintaining all its functionalities. The uplink data-rate is fixed at 4 kbits/s whereas downlink data-rate has a maximum capability of 838 kbit/s [8], as already seen in the previous paragraph. In this mode three possible types of data may be transmitted:
 - HKTM-P, which are information on the current state of the satellite and must always be transferred to the ground station, when in visibility and with the emitter is switched on;
 - HKTM-R, which provide history of recent data on the satellite. This data is stored on board and can be transmitted upon request from the ground station;
 - PLTM, which is also stored on board on a dedicated internal mass memory of 2 Gbits, until a ground station enters the satellite's Field of View (FOV) and it can be transferred.
- During orbital maneuvers the satellite maintains full operability, however, since the control is obtained through thrusters aligned with the +X satellite axis, the satellite is reoriented during this phase so data acquisition through the payload might not be possible.
- In case of emergency the satellite enters in the Safe Hold Mode (SHM), with the objective of reaching a safe attitude with the -X satellite axis pointed to the Sun. In this mode the satellite TM is reduced only to essential data, but its receiver is always on to receive TC and start to transition to another mode.

3.3 Reverse Sizing

In this section a preliminary reverse sizing of the TTMTTC subsystem will be discussed taking into account its most important aspects.

3.3.1 Losses

The channel losses computation is composed of four distinct types of contributions. Free space, pointing, cable and atmospheric losses have been taken into account.

Free space losses account for the distance between the satellite and the Ground Station. The sizing is performed at the worst case, which is at maximum distance, using the frequency from Table 3.1 as $f_{uplink} = 2040.343$ MHz and $f_{downlink} = 2214.92$ MHz:

$$L_{free\ space} = 20 \cdot \log_{10} \left(\frac{c}{4\pi \cdot f \cdot r} \right) \quad [dB] \quad (3.1)$$

where c is the speed of light, f is the wave frequency, r is the maximum distance of the spacecraft from Earth, which is 1370 km.

Pointing losses, which account for the pointing accuracy and receiver beam-width are defined as:

$$\begin{cases} L_{pointing} = -12 \cdot \left(\frac{\eta_p}{\theta_{rx}} \right)^2 \quad [dB] \\ \theta_{rx} = 70 \cdot \frac{c}{f \cdot D} \quad [deg] \end{cases} \quad (3.2)$$

where D is the antenna diameter and η_p is the pointing efficiency. The transmitter and receiver couple is selected from Table 3.2 to simulate the worst-case scenario with the largest antenna diameter and highest losses. For the downlink, a diameter of 21 meters is used, corresponding to NOAA's Fairbanks Command and Data Acquisition Stations[14]. For the uplink, RUAG's S-band Helix TTC Antennas[18] are utilized. The pointing accuracy for the uplink MGA antenna was assumed to be 0.1 while for the downlink receiver antenna the accuracy was assumed 0.05 due to the precise pointing capabilities of the CDAS antenna.

Position	Antenna	Diameter	Receive Bands	Transmit Bands	Efficiency	θ_{rx} [deg]	L_{point} [dB]
Wallops (USA)	18 METER A [23]	18 m	S	S	0.55	0.5264	-0.1083
Usingen (GER)	USG-2 [10]	13 m	No data	No data	0.55	0.73	-0.0565
Fairbanks (USA)	21 METER [14]	21 m	L/S	S	0.55	0.4512	-0.1474
Satellite	Raug Helix [18]	65 mm	S	S	0.7	158.23	$-4.79 \cdot 10^{-6}$

Table 3.2: Technical Specifications for the largest dish of each Ground Station and Satellite

Through graphical analysis we can assume the atmospheric losses around $L_{atm} = -0.04$ dB and cable losses are assumed to be $L_{cab} = -2$ dB. Table 3.3 shows the main signal losses of the system.

3.3.2 Antennas

The antennas used for both downlink and uplink are analysed in the following paragraph. The gain for both antennas is obtained through the formula:

$$G = 10 \cdot \log_{10} \left(\mu \cdot \left(\frac{\pi \cdot D \cdot f}{c} \right)^2 \right) \quad [dB] \quad (3.3)$$

where μ is the antenna efficiency, which is $\mu_{helix} = 0.70$ for helix antennas and $\mu_{para} = 0.55$ for parabolic antennas. The gains for the receiver and for the transmitter antennas has been calculated for all frequencies used and is reported in the following Table 3.3.

	$L_{freespace}$	$L_{Pointing}$	L_{atm}	L_{cable}	G_{tx}	G_{rx}
Downlink	-162.089	-0.147	-0.04	-2	2.023	51.162
Uplink	-161.376	$-4.792 \cdot 10^{-6}$	-0.04	-2	50.449	1.310

Table 3.3: Uplink and downlink signal losses, transmitter and receiver gains [dB]

The system noise density N_0 related to the receiving antenna can be computed as $N_0 = 10 \cdot \log_{10} (kT_s)$

where k is the Boltzmann constant ($1.38 \cdot 10^{-23} \text{ Ws/K}$) and T_s is the system temperature, which was assumed to be $T_s = 250.35 \text{ K}$ for the Fairbanks CDAS as this was the lowest average monthly temperature [4], while for the Jason-2's antenna it was assumed to be $T_s = 233.15 \text{ K}$ as it was indicated as the lowest temperature for operational payload systems. [8]

The noise density can now be computed: for the downlink receiver antenna $N_0 = -204.616 \text{ dB}$ while for the uplink receiver antenna $N_0 = -204.925 \text{ dB}$.

3.3.3 Amplifier

As no information on the amplifier used was found on the documentation, it was assumed the use of a Solid State Amplifier (SSA). This was done mainly because of two reasons: the SSA is usually preferred at the frequencies used (2GHz) and the scientific payload of the Jason-2 mounted a SSA as well.

It was assumed the use of a largely used amplifier in Jason-2's period such as the Airbus Defence and Space S-Band SSA with an output power of $P_{tx} = 15 \text{ W}$ and an efficiency of $\mu_{amp} = 0.31$ [63]. From this the power input can be computed as:

$$P_{in} = \frac{P_{tx}}{\mu_{amp}} = 48.387 \text{ W} \quad (3.4)$$

Knowing from the PROTEUS User's Manual [26], the power budget for the bus is 300 W, which means that an input power of almost 50 W for the TTMTTC System is an acceptable estimate.

For the ground station, the smallest power output of all antennas was selected as a worst case scenario. The power output used for the ground station is $P_{tx} = 50 \text{ W}$.[2]

3.3.4 Link Budget

To calculate the link budget a Bit Error Rate (BER) has to be selected. For TM and downlink a BER of 10^{-5} was selected, while for the TC a higher BER of 10^{-7} was selected to guarantee higher accuracy.

For QPSK modulation $\alpha_{mod} = 2$ while for Reed-Solomon and convolutional encoding ($k = 7$ and rate = 1/2) which translates in an encoding coefficient $\alpha_{enc} = 2.2869956$.[64]

$$R_{data\ real} = R_{data} \frac{\alpha_{enc}}{\alpha_{mod}} = 958.25 \text{ kbit/s} \quad (3.5)$$

With the BERs obtained earlier, the necessary error per bit to noise density ratio is $\frac{E_b}{N_0} = 5.5 \text{ dB}$ for downlink and $\frac{E_b}{N_0} = 6 \text{ dB}$ for uplink. To this a 3 dB margin is added, as per ESA regulations. The system's error per bit to noise density ratio can be computed as:

$$\frac{E_b}{N_0} = 10 \cdot \log_{10} (P_{tx}) + G_{tx} + G_{rx} + L_{total} - N_0 - 10 \cdot \log_{10} (R_{data\ real}) \quad [\text{dB}] \quad (3.6)$$

From this equation the link budget for both downlink and uplink is extensively verified with $(\frac{E_b}{N_0})_{down} = 80.698 \text{ dB}$ and $(\frac{E_b}{N_0})_{up} = 98.425 \text{ dB}$, which means that the system is suitable for its required applications in the worst case scenario.

It is necessary to verify if the receiver is capable of tracking the signal and distinguishing it from the noise. This requires ensuring that $SNR_{margin} = SNR_{carrier} - SNR_{minimum} > 3 \text{ dB}$. By selecting $SNR_{minimum} = 10 \text{ dB}$, $SNR_{carrier}$ must be calculated using the following relation:

$$SNR_{carrier} = P_{tx} + G_{tx} + G_{rx} + L_{tot} + P_{mod,loss} - N_0 - 10 \log(B) \quad (3.7)$$

where P_{tx} is the transmitter power, G_{tx} and G_{rx} are the gains of the transmitter and receiver respectively, L_{tot} represents the total losses, B is the bandwidth, N_0 is the noise power density and $P_{mod,loss} = 20 \log(\cos(\beta_{mod}))$, assuming the modulation index $\beta_{mod} = 78$ degrees. First, the bandwidth must be calculated using the formula $B = R_{real}(1 + \alpha) = 1.29 \text{ MHz}$, where $\alpha = 0.35$ is the roll-off factor which depends on the modulation filter[28]. This results in two values both compatible with the system margin: $SNR_{margin,uplink} = 53.507 \text{ dB}$ and $SNR_{margin,downlink} = 88.763 \text{ dB}$.

Assignment 4

Attitude Dynamics and Control Subsystem

Change Log	
§ 4.2	pp 33: Table 4.3 revised
§ 4.3	pp 33: Introduction paragraph to pointing budget revised and addition of source citations pp 34: Addition of Table 4.4 pp 34: Addition of Figure 4.4's explanation and context
§ 4.5.1	pp 36: Addition of details and motivation for the choice for the desaturation duration

4.1 Architecture

Jason-2 is a Nadir-pointing, three-axis stabilized satellite. The spacecraft's attitude is held in place by reaction wheels and magnetic torque rods, while a hydrazine propellant system is used for precise orbital maintenance and station keeping. The system is mounted on the PROTEUS platform, which also has the capability to control the Attitude and Orbit Control System (AOCS) system. Figure 4.1 shows the positioning of the various components inside the PROTEUS platform.

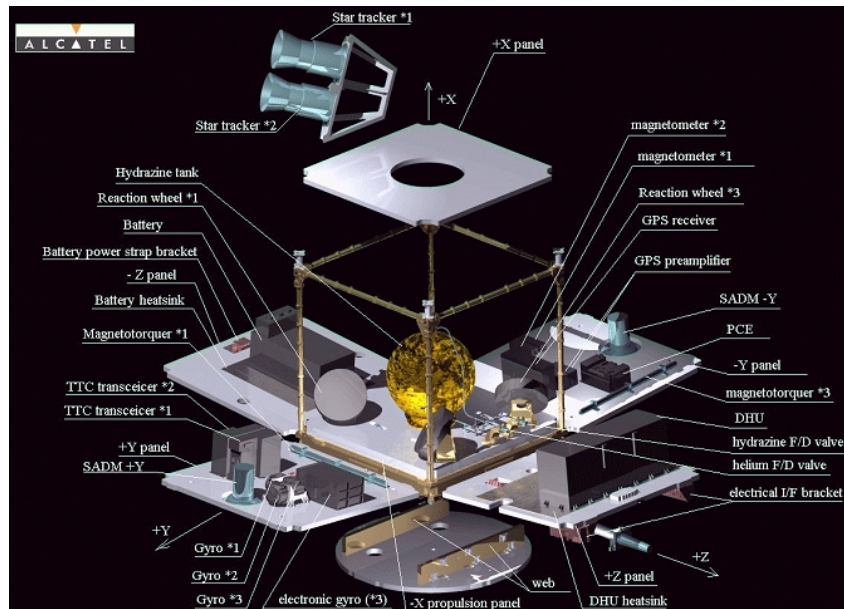


Fig. 4.1: Proteus Platform Exploded Assembly Drawing

In order to achieve a data acquisition accuracy of 33 mm [8], the Jason-2 satellite must be equipped with a very precise Attitude and Orbit Control System to ensure the high pointing accuracy required. The PROTEUS

platform guarantees a stability of 0.0007 deg/s at low frequencies ($< 1 \text{ Hz}$) and high pointing accuracy of 0.05° , with the addition of a further 0.05° as a pointing bias for all axis [50]. Furthermore, Jason-2 is able to determine its orbit position through an integrated GPS system mounted on board, achieving a precision of around 120 meters [26]. Additional systems, such as the Precise Orbit Determination (POD) payloads, are used to improve the satellite's orbit determination capability even more, reaching an impressive sub-meter precision [8]. This accuracy allows Jason-2 to fly during nominal mode in a Nadir pointing position, aligning all its instruments towards Earth.

Due to its particular orbit, the position of the sun with respect to the satellite continuously varies during a full revolution of the spacecraft, requiring careful management of the satellite's power systems. To ensure a continuous power supply, the solar array is equipped with an independent driver known as the Solar Array Drive Mechanism (SADM). This mechanism is coupled with a yaw steering movement, which is used to orient the solar array towards the sun, as depicted in Figure 4.3, thus minimizing thermal and power losses. Throughout the entire charging operation, the $+Z$ satellite axis remains pointed towards the Nadir axis.

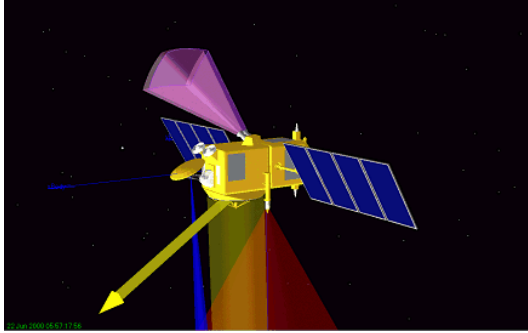


Fig. 4.2: 3D illustration of Jason2's attitude determination by PRESTO

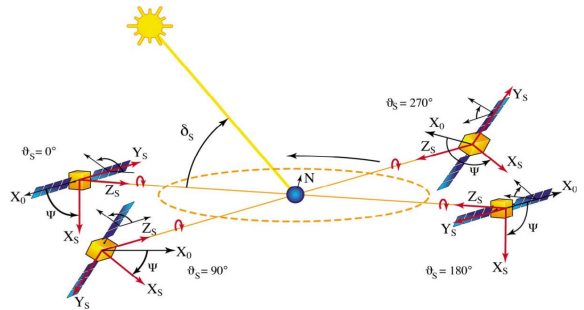


Fig. 4.3: Yaw steering correction for solar panels

For missions such as the OSTM Jason-2, which are designed to operate almost continuously for at least 3 to 5 years, reliability is absolutely crucial. Therefore, most of the sensors and actuators on board of the satellite have one or more copies implemented for redundancy.

4.1.1 Sensors

The sensor set of the Jason-2 is composed of two 3-axis star trackers (STR), three 2-axis gyroometers (GYR), two 3-axis magnetometers (MAG), eight coarse sun sensors (CSS), and a GPS for orbit positioning. These sensors include all the copies implemented on the spacecraft for redundancy.

The Star Tracker Array (STA) is composed of two CALTRAC® Star Trackers produced by EMS Technologies Inc., one for nominal use and one for cold redundancy, and the structure containing the star trackers, which is coated in Multi Layer Insulation (MLI) and Secondary Surface Mirrors (SSM) for thermal and radiological protection [26]. The star trackers have a maximum power usage of 14 W and a mass of 3.4 kg each [41], while the whole STA has a total mass of 11.4 kg [26].

The baseline gyro array (GYR) consists of three 2-axis gyros and their respective electronics. Due to the extensive utilization throughout all the Jason-2 control modes, a fully redundant configuration was selected, in which only two gyros out of three operate in nominal mode. The gyros are mounted in an orthogonal configuration on the spacecraft, thus providing redundant measurements on all spacecraft axis. These sensors are the baseline error sensors for all modes except survival mode [50]. The REGYS 3S Dynamically Tuned Gyroscope (DTG) were the sensors used in this mission and were manufactured by Sagem, now known as Safran.

The Coarse Sun Sensor (CSS) set consists of 8 analog solar cells mounted on the spacecraft to provide a 4-pi steradian coverage, allowing $360 \times 180^\circ$ visibility. The analog sun sensors provide a current output proportional to the cosine of the sun angle with respect to the normal of the solar cell. Along with the magnetometers, the CSS are used as the control sensors during survival mode and are used to provide initial attitude determination during the stellar acquisition process [50]. The loss of only one out of eight solar cells is permitted to maintain nominal functioning. The analog solar cells are manufactured by Adcole Maryland Aerospace and are grouped into two arrays of 4 cells each, one for the Pitch axis and one for the Yaw axis, weighing 0.13 kg each [27].

The PROTEUS baseline design contemplated a non-redundant configuration for the magnetometer, but for longer missions, such as Jason-2, it was decided to implement a second magnetometer for cold redundancy and to improve reliability. This sensor provides measurement of the local Earth magnetic field, which is used during survival mode

and initial attitude determination. Additionally, it is used during Star Acquisition Mode to provide momentum management control signals. To ensure a proper reading of the Earth's magnetic field, all magnetic torquer bars will not be commanded during measurement; this is done to prevent the formation of a spacecraft-developed magnetic field [50]. The magnetometer used on the Jason-2 satellite was the IM-103 produced by Ithaco Space Systems, which has a power usage of 0.95 W and a mass of 0.231 kg [40].

The baseline sensor set did not include the use of GPS, however it was implemented on Jason-2 to validate its use as an attitude determination system. This was done by comparing the results obtained with the STR with the GPS data during all operational modes [50]. The GPS mounted on the PROTEUS platform was developed and manufactured by Laben, which is now part of Thales Alenia Space.

In Table 4.1 the main data from each sensor is presented.

	Number	Redundancy	Mass [kg]	Power [W]	FOV	Accuracy	Range
STR	2	1 + 1	3.4	14	22° x 18°	±0.013° for Pitch/Yaw ±0.035° for Roll	/
GYR	3	2 + 1	/	/	/	/	/
CSS	8	1 Failure Allowed	0.13	0	360° x 180° (4-Pi Steridian)	±1° at null ±5° in linear range	500 - 1300 μA
MAG	2	1 + 1	0.231	0.95	/	±4 mG	±600 mG

Table 4.1: Sensor Data

The total mass of the sensor set is 8.3 kg while the total power usage is 29.9 W.

4.1.2 Actuators

The attitude control of Jason-2 is done with a set of 4 reaction wheels which are desaturated with 3 magnetic torque bars.

The reaction wheels used in the Proteus Bus are the RSI 8-120/351 manufactured by Teldix (now Collins Aerospace) [35]. They have a torque of 0.075 Nm, a momentum at nominal speed of 8 Nms and operational speed range of ±3500 rpm, they are usable as both momentum and reaction wheels [50] [17]. Four reaction wheels are used in a pyramidal configuration [50] as it allows the loss of a single reaction wheel without affecting the mission, furthermore the satellite can go into its Safe Hold Mode with only one operational reaction wheel [35].

The magnetic torque bars used in the Proteus Bus are the TR60CFR manufactured by Ithaco Space Systems (now Collins Aerospace) [40] [50] [19]. They have a linear dipole of 60 Am², a residual dipole of 0.7 Am² and a weight of 1.7 kg. They have high redundancy as each magnetic torque bar has a nominal and a redundant coil [35].

The orbit control of Jason-2 is done with a set of 4 1N hydrazine thrusters. The 1N thrusters were manufactured by Astrium (now Airbus Defence and Space), with a thrust of 0.32 – 1.1 N, specific impulse 200 – 223 s and minimum impulse bit 0.01 – 0.043 Ns [1]. All four thrusters are pointed in the same direction, this provides redundancy as OCM2 is guaranteed to work with the loss of any single thruster and could still work if two thrusters are lost as long as they are diagonal to each other.

	Number	Redundancy	Mass [kg]
Reaction Wheels	4	3 + 1	—
Magnetic Torque Bars	3	1 Redundant Coil on each Bar	1.7
Thrusters	4	1 Failure Allowed (loss of OCM4)	0.29

Table 4.2: Actuator Data

The total mass of the actuator set is 6.26 kg.

4.2 Control modes

Jason 2 employs a range of control modes to manage its operations effectively, ensuring mission objectives are achieved while maintaining safety and functionality.

Start-up (LUM)

The Attitude and Orbit Control System is completely empowered during launch. This mode is referred as Launch Mode (LUM).

Safe Hold Mode (SHM)

This mode is vital for ensuring the satellite's safety and stability in various scenarios and is often referred to as Survival

Mode. SHM is activated in case of detection of anomalous condition or hardware failure. Moreover this mode is used to acquire the initial attitude after separation with the launcher. SHM consists of three main phases: Rate Damping Phase (RDP), Sun Pointing Phase (SPP), and Barbecue Phase (BBQ). The primary goal of SHM is to autonomously achieve a safe attitude configuration, detumbling from launch rotation, and then orienting with the -X satellite axis directed towards the Sun at a mean roll angular rate of $-0.25^\circ/\text{s}$. During the BBQ phase, the satellite slowly rotates in space to achieve an even temperature distribution under solar radiation. In this mode, PROTEUS provides the minimum satellite management needed to support vital functions for diagnosis or anomaly handling. These functions include ground-to-satellite communication, thermal control, battery management, failure management, and reduced payload power 30W. Coarse Sun Sensors and Magnetometers are used for attitude measurement, while Magnetic Torquer Bars generate torque. Additionally, two of the four reaction wheels are utilized to provide gyroscopic stiffness.

Star Acquisition Mode (STAM)

This mode is instrumental in reacquiring fine attitude, position, and time information during the transition from Safe Hold Mode to Nominal Mode. It begins when the satellite is considered safe and is engaged upon receiving a ground command while in SHM. During STAM, payload operations are restricted to verifying instrument behavior, with priority given to housekeeping operations. Typically, the nominal payload is turned off, but if necessary, two of the sixteen power lines can be maintained on to ensure payload power reduced to 30W.

Nominal Mode (NOM)

Nominal Mode facilitates essential satellite management functions and provides generic or specific services required by the payload, where the scientific missions are performed. This mode includes power distribution, commanding, status monitoring via the Mil-STD-1553B bus, precise data acquisition, and fine pointing. Nominal Mode can be engaged in various ways, including transitioning from Star Acquisition Mode upon ground request, automatically when leaving the OCM, or through a NOM reset process initiated by ground request for equipment configuration changes. In this phase, the spacecraft is inertially stabilized using the reaction wheels, while attitude is maintained with a precision in the order of arcseconds through Kalman filtering of Star Tracker and GYR data. During NOM, any excess momentum accumulated in the reaction wheels due to external disturbance torque is dissipated magnetically using Magnetic Torquer Bars (MTB).

Satellite OCM Modes

Orbit Control Mode (OCMs) are essential for executing orbit adjustments effectively. While their performance and services resemble Nominal Mode, attitude pointing may be affected, and payload functioning may be restricted during significant maneuvers.

- OCM2 is used for moderate orbit adjustments with only two thrusters, ensuring control without major disruptions.
- OCM4 handles significant maneuvers using all four thrusters, as the maneuvers performed require more precision.

The choice of which OCM to utilize depends on mission objectives and the magnitude of the required orbit adjustments. These modes are engaged upon ground request, always transitioning from the Nominal Mode. They automatically transition back to Nominal Mode when the orbit maneuver is completed or transition to Start-up Mode in case of any alarm.

The use of the components of the AOCS in each mode is summarized in Table 4.3.

	LUM	SHM	STAM	NOM	OCM2	OCM4
Gyro	OFF	ON (not used)	ON	ON	ON	ON
Star Tracker	OFF	OFF	ON	ON	ON	ON
Coarse Sun Sensor	OFF	ON	ON	ON (not used)	ON (not used)	ON (not used)
Magnetometer	OFF	ON	ON	ON	ON	ON
Reaction Wheels System	OFF	ON	ON	ON	ON	ON
Magnetic Torquer Bars	OFF	ON	ON	ON	ON	ON
Thrusters	OFF	OFF	OFF	OFF	ON (only 2)	ON (all 4)
GPS	OFF	ON	ON	ON	ON	ON

Table 4.3: **Hardware utilization** in each mode [50].

4.3 Pointing Budget

In nominal operational mode, the pointing budget is mainly driven by the accuracy requirements of the scientific instruments on board, as discussed in section 4.1. The precision of pointing shall meet a minimum of 0.15° (3σ), and the knowledge of pointing shall be within 0.05° of the pointing axis, with a bias of less than 0.05° (3σ) [50].

The total pointing requirements of the Jason-2's subsystems are summarised in Table 4.4. As said earlier, the most constraining requirement is the pointing precision of the payload scientific instrumentation and most of the other subsystems require a precision a order of magnitude higher. The data reported in Table 4.4 was found on the Proteus's User Manual [26] or, when no data was available, it was reasonably assumed from the pointing budgets of similar LEO missions satellites.

Phases	LEOP		Assesment and Verification Phases				Operational and Extended Phases			
	SHM	OCM	SHM	STAM	NOM	OCM	SHM	STAM	NOM	OCM
TTMTC	AKE = 2° APE = 5°	AKE = 1° APE = 3°	AKE = 2° APE = 5°	AKE = 0.5° APE = 2°	AKE = 0.5° APE = 2°	AKE = 0.5° APE = 2°	AKE = 2° APE = 5°	AKE = 0.2° APE = 1°	AKE = 0.2° APE = 1°	AKE = 0.2° APE = 1°
PS	-	AKE = 1.5° APE = 3°	-	-	-	AKE = 0.2° APE = 0.5°	-	-	-	AKE = 0.2° APE = 0.5°
EPS	AKE = 5° APE = 40°	AKE = 5° APE = 40°	AKE = 5° APE = 40°	AKE = 3° APE = 25°	AKE = 3° APE = 25°	AKE = 3° APE = 25°	AKE = 5° APE = 40°	AKE = 3° APE = 25°	AKE = 3° APE = 25°	AKE = 3° APE = 25°
PL	-	-	AKE = 0.5° APE = 1.5°	AKE = 0.05° APE = 0.15°	AKE = 0.05° APE = 0.15°	-	AKE = 0.5° APE = 1.5°	AKE = 0.05° APE = 0.15°	AKE = 0.05° APE = 0.15°	-

Table 4.4: Jason-2's pointing budget divided in subsystems for each phase and mode

It is worth mentioning that the final annual report [34] details the pointing precision of the satellite in its final phase. The system achieved an average precisions below 0.005 degrees from nadir pointing, compared to 0.07 degrees in the first year [43]. Notably, the requirement was 0.2 degrees, indicating that the AOCS overperformed and improved throughout the mission. In Figure 4.4 the actual pointing performances of the satellite are visually shown in time, throughout the extended phase.

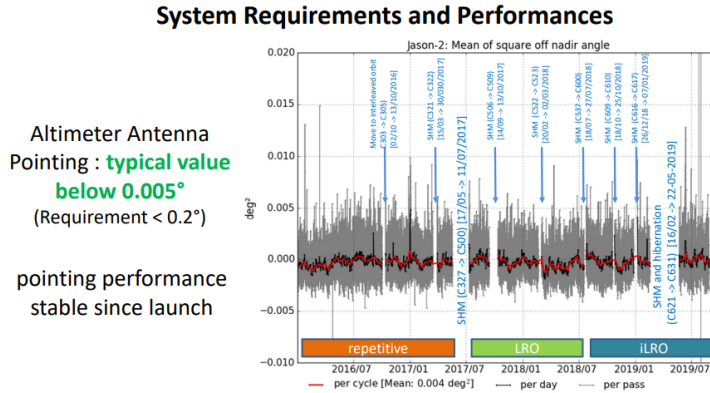


Fig. 4.4: Pointing Performances in the extended phase

4.4 Disturbances

A satellite in an Earth-centered orbiting mission is subject, during its operational life, to several environmental disturbance torques. Counter acting the attitude disturbances coming from the environment is crucial in order to pursue the scientific objectives of the mission and to perform the attitude control's operations.

In the particular case of Jason-2 the disturbances which have a bigger impact on the spacecraft are: Atmospheric Drag, Gravity Gradient, Solar Radiation Pressure (SRP), and Magnetic Moment. The disturbance are calculated in the worst case scenario for each disturbance and then a 100% margin is applied for safety.

Atmospheric Drag

The Atmospheric Drag is a disturbance caused by the collision of the spacecraft with air particles coming from the atmosphere and it is constant for Earth-pointing satellites, such as Jason-2.

To calculate the torque created by the Atmospheric Drag, the following formula is used:

$$T_{AD} = \frac{1}{2} \rho C_D A v^2 (c_p - c_g) \quad (4.1)$$

ρ is the air density at the desired altitude;

C_D is the drag coefficient of the the spacecraft, which is 2.75 at Jason's 2 altitude [26];

v is the velocity of the spacecraft, which is computed knowing the orbital parameters and is equal to 7188.3 m/s;

A is the spacecraft's relative area with respect to the velocity vector, which, knowing the spacecraft's mass-to-area ratio and the satellite's mass [26], can be computed as $\sim 5 m^2$;

$(c_p - c_g)$ is the difference between the center of aero pressure and the center of mass, which was assumed to be 0.5 m.

Gravity Gradient

Gravity Gradient is a disturbance caused by the effect of gravity on different parts of the spacecraft and it is constant for Earth-pointing satellites.

To calculate the torque created by the Gravity Gradient, the following formula is used:

$$T_{GG} = \frac{3\mu}{2R^3} (I_{max} - I_{min}) \sin(2\theta) \quad (4.2)$$

μ is the standard gravitational parameter of Earth, which is $3.986 \cdot 10^{14} m^3/s^2$;

R is the radius of the satellite's orbit, which is 7714 km;

$(I_{max} - I_{min})$ is the difference between the maximum and minimum moment of inertia, which is $705.1 - 321.2 = 383.9 m^2 kg$ [61];

θ is the max deviation of the Z axis with respect to the local vertical, which is assumed to be 45° as a worst case scenario.

Solar Radiation Pressure

The Solar Radiation Pressure is a disturbance caused by the interaction of solar radiation particles with the surface of the spacecraft and it is cyclic for Earth-pointing satellites.

To calculate the torque created by the Solar Radiation Pressure, the following formula is used:

$$T_{SRP} = \frac{F_s}{c} A_s (1 + q) \cos(I) (c_{sp} - c_g) \quad (4.3)$$

F_s is the solar constant at spacecraft distance, which is $1367 W/m^2$;

c is the speed of light, which is $2.997 \cdot 10^8 m/s$;

A_s is the relative area with respect to the direction of the Sun which is $3.105 m^2$ for the main body of the spacecraft and $9.8 m^2$ for the solar array [5];

q is the reflectance factor, which is 0.246 for the main body of the spacecraft and 0.098 for the solar array [5];

I is the incidence angle of the solar radiation particles, which for worst case scenario is assumed to be 0° ;

$(c_{sp} - c_g)$ is the difference between the center of solar radiation pressure and the center of mass, which was assumed to be 1 m for the solar array and 0.5 m for the main body of the spacecraft.

Magnetic Moment

The Magnetic Moment is a disturbance caused by the interaction of Earth's magnetic field with the spacecraft and it is cyclic for Earth-pointing satellites.

To calculate the torque created by the Magnetic Moment, the following formulas are used:

$$T_{MAG} = D \cdot B \quad (4.4) \qquad B = \frac{2M}{R^3} \quad (4.5)$$

D is the residual dipole of the spacecraft, which is assumed to be $5 Am^2$ [40];

B is the value of Earth's magnetic field at a certain altitude;

M is Earth's magnetic moment, which is $7.96 \cdot 10^{15} Tm^3$;

R is the radius of the satellite's orbit, which is 7714 km;

The total disturbance values are reported in Table 4.5.

Disturbance	Type	Value
Atmospheric Drag	Constant	$1.776 \cdot 10^{-7} \text{ Nm}$
Gravity Gradient	Constant	$5.000 \cdot 10^{-4} \text{ Nm}$
SRP	Cyclic	$5.789 \cdot 10^{-5} \text{ Nm}$
Magnetic Moment	Cyclic	$7.283 \cdot 10^{-5} \text{ Nm}$
	Total	$6.309 \cdot 10^{-4} \text{ Nm}$
	With Margin	0.0013 Nm

Table 4.5: Mean disturbance values

4.5 Reverse Sizing

4.5.1 Reaction Wheels

The reaction wheels provide attitude control to the spacecraft by counteracting the external disturbances and performing slew maneuvers and are sized accordingly to perform and accomplish these tasks.

Station Keeping

As seen in section 4.4, the total disturbances acting on the satellite, considering a 100% margin, are $T_{tot} = 0.0013 \text{ Nm}$. The total angular momentum generated by the disturbances can be computed as:

$$h_{dis} = T_{tot} \cdot T_p = 0.0013 \cdot 6720 = 8.736 \text{ Nms} \quad (4.6)$$

Where T_p is the period of the orbit, which is 6720 s.

Knowing that the angular momentum of each wheel at nominal speed is 8 Nms, which means that the reaction wheels saturate in ~ 3 orbits.

Slew Maneuver

Assuming a maximum slew rate of 0.5 °/s (0.25 °/s in SHM) and a slew angle of 180°, as a worst case scenario, the torque needed can be easily computed with the following formula:

$$T_{RW} = N_{RW} \theta_{max} \frac{I_{max}}{t_{min}^2} \quad (4.7)$$

Where t_{min} is the minimum time to perform the maneuver, knowing the maximum slew rate, in this case $t_{min} = 360 \text{ s}$ (720 s in SHM).

The torque required by each reaction wheel to perform a 180° slew at maximum slew rate is $T_{RW} = 0.0684 \text{ Nm}$ (0.0171 Nm in SHM), which is lower than the maximum available torque of each reaction wheel (0.075 Nm).

4.5.2 Thrusters

Slew Maneuver

Assuming the same maximum slew rate of 0.5 °/s (0.25 °/s in SHM) and slew angle of 180° as earlier, the torque needed by the thrusters can be easily computed with the following formula:

$$T_{th} = \frac{I_{max} \theta_{max}}{n_{th} L t_{min}^2} \quad (4.8)$$

Where L is the distance between the thruster and the centre of gravity, which is 0.845 m [61].

Using 2 thrusters in Nominal Mode the thrust needed by each thruster is 0.0101 N, which is just over the minimum impulse of each thruster (0.01 N) [1]. For Safe Hold Mode and Nominal Mode using 4 thrusters the thrust required by each thruster is too low, thus making any slew maneuver using thrusters not possible.

Reaction Wheel Desaturation

Reaction Wheels desaturation can be performed either passively by changing the solar panel orientation, to exploit Solar Radiation Pressure, or actively by firing a set of thrusters or using magnetic torquers. the last option is usually the preferred option, but in this paragraph we will explore the possibility of using thrusters for desaturation. This maneuver is usually performed with only 2 thrusters, as it's considered a secondary maneuver, but in this section the possibility of using 4 thrusters is explored as well.

Given the high precision requirements, the reaction wheels must desaturate in often with short durations. For this reason a desaturation time of 30 s was assumed, as seen in missions with similar precision requirements and objectives. The required thrust from each thruster can be computed with the following formula:

$$T_{th} = \frac{h_{RW}}{n_{th} L t_{des}} \quad (4.9)$$

The required thrust using two thrusters is $T_{th} = 0.6312 N$, while using four thrusters is $T_{th} = 0.3156 N$. These values are acceptable, since both are lower than the maximum amount of thrust which can be produced [1].

Propellant Mass Budget

It is possible to compute the propellant mass by combining the duration of each momentum dump manoeuvre and the total number of dumps required according with the following equation:

$$m_p = n_{des} \frac{t_{des} T_{th}}{I_{sp} g_0} \quad (4.10)$$

Where I_{sp} is the specific impulse, which is 220 s [1]. Considering the total mission time of 11 years, the number of desaturations maneuvers to perform is 718, considering a 20% margin.

The total propellant mass which would be used to desaturate the reaction wheels is 0.1 kg using two thrusters and 0.05 kg using 4 thrusters, which are acceptable values considering the 28 kg fuel tank.

Assignment 5

Thermal Control Subsystem

5.1 Architecture

Understanding how the Thermal Control System (TCS) design of PROTEUS was dimensioned is critical to advance in the analysis of the Jason-2 mission. This subsystem was designed to withstand the required maximum thermal loads with margins, relying on both passive regulation, such as radiators, and active regulation through the use of heaters.

OSTM/JASON 2 mission consists of two main components: the Proteus platform and the payload module. The bus system has been equipped with various solutions to regulate system temperature effectively and maintain operational stability. Additionally, in order to ensure payload safety and health, PROTEUS provides thermal control and heater power to the payload in all satellite modes.

It is noteworthy that PROTEUS has been designed to meet the versatile demands of different missions. For this reason, the generic design of this platform must endure a wide range of environments, with orbits spanning altitudes from 500 to 1500 km and various inclinations. These requirements impose strict demands on the Thermal Control System, which must keep all equipment within specified temperature ranges despite significant fluctuations in thermal loads [26].

To address these challenges, a passive thermal control design has been adopted, featuring strategically positioned radiators aided by a software-controlled active heater system.

The thermal control components used on Proteus are:

- External and internal Multi Layer Insulation (MLI)
- Heater lines and thermistors
- Silvered Secondary Surface Mirrors (SSM) Radiators
- Thermal straps and insulating washers
- Aluminium doublers, which spread heat in the radiators.
- White paint on the dedicated cylindrical radiator of the launcher adaptor.

The active regulation uses heaters located on the panels of the platform (or on some specific equipment, such as the battery) and is monitored by the on-board computer. Temperature sensors located nearby the electric heaters send to the computer the difference from the set-point temperature. Consequently, this computer applies the power needed to reach the operational target.

The thermal control of Jason-2 is divided into 5 distinct parts each one as much uncoupled as possible from the others: [42]

1. Battery zone
2. Propulsion panel
3. Main platform zone, excluded Battery and Propulsion
4. Star Tracker Array (STA)
5. Payload Module, including scientific instruments

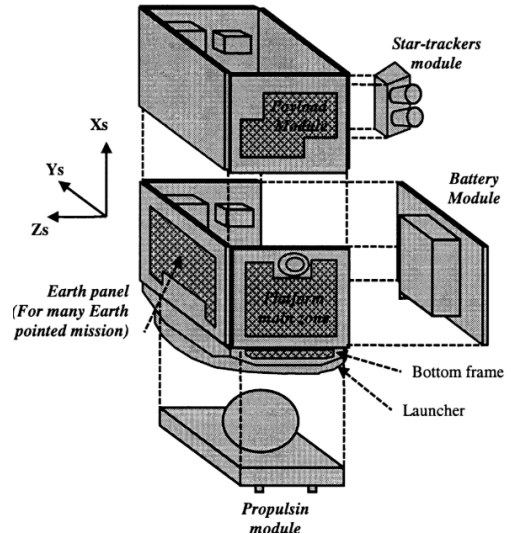


Fig. 5.1: TCS Components' Design

In order to ensure efficient thermal decoupling between the PROTEUS platform and its payload, four mechanical links that are situated on the upper faces of four pods act as an interface.

Figure 5.2 depicts the payload module of Jason-2, which has a cubical shape with no central structure, mirroring the platform's structure. The cube's panels serve as both structural support and heat rejection surfaces for module thermal control.

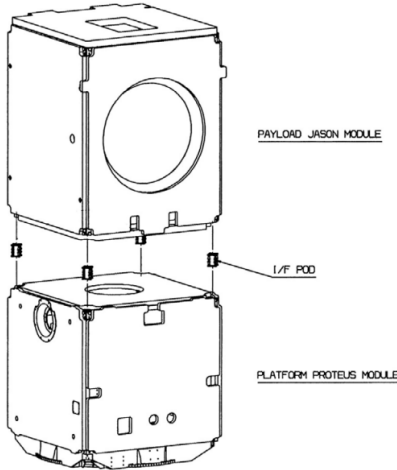


Fig. 5.2: Interface PROTEUS - Payload

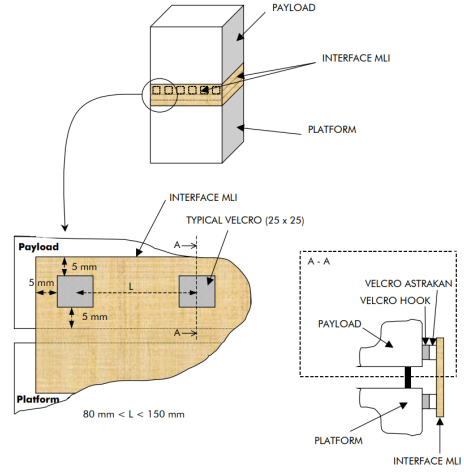


Fig. 5.3: MLI Interface between Platform and Payload

5.1.1 Multi Layer Insulation (MLI)

Multi Layer Insulation (MLI) consists of a very lightweight reflective film assembled in many thin layers, typically made of polyimide or polyester films. Typically, MLI can guarantee a reflection of up to 95% of radiation away from the spacecraft, depending on the number of layers. [13]

Multi Layer Insulation is one of the main components of PROTEUS's passive thermal control and can be used both internally and externally on various sections of the spacecraft. MLI is present in the following satellite elements:[42]

- In the battery module, which, due to its specific low and narrow temperature range, is decoupled from the rest of the platform through the presence of an internal MLI coating.
- Inside the propulsion zone, an internal layer of Multi Layer Insulation (MLI) is placed on the tank, on the upper side of the -Xs panel, and on all hydrazine-rich components located on the upper side of the propulsion panel, to limit radiative coupling with the platform.
- The entire main zone of the platform is covered with a layer of MLI, except for radiative surface areas, as well as all external areas of the satellite, excluding those requiring a line of sight with the Sun and Earth.

5.1.2 Heater Lines and Thermistors

Electric resistance heaters are composed of a polyimide film with etched foil circuits that generate heat when a current is applied. [21]

In the PROTEUS satellite, active thermal regulation utilizes electric heaters positioned on the platform panels and specific equipment. The performance of the regulation depends on the main characteristics of the heating lines, which may vary depending on the components or areas heated. The thermal stability of the lines can be summarized as: [42]

- Approximately 0.3°C on heating lines with low thermal inertia and sensors located near the heaters.
- Approximately 0.5°C on heating lines with high thermal inertia and sensors located near the heaters.
- Approximately 1.0°C on heating lines with high thermal inertia and sensors located far from the heaters.

On the PROTEUS Platform, 11 nominal and 11 redundant heating lines are used, each associated with three temperature acquisition sensors. For active thermal control, another additional 33 acquisition lines are used, along with thermal sensors compatible with these lines. [26]

In particular, the sensors utilized include the Fenwal 526-31 BS12-153, which is a thermistor that has a temperature measurement range from -60°C to +90°C, and the Rosemount 118 MF, a sensor with measurement has a range from -120 °C to +140°C. [26]

5.1.3 Silvered SSM Radiators

A radiator is a surface with low solar absorptivity and high infrared emissivity that is intended to dissipate excess heat through radiative heat transfer.

In Secondary Surface Mirrors Radiators, incident light enters the front surface, passes through a substrate of teflon or glass, and reflects off the coating of the back surface, also known as second surface, which in this case is made out of silver. The substrate serves primarily to provide a smooth, transparent surface to support and safeguard the reflective coating. Typically, a Secondary Surface Mirrors reflects 80% to 85% of incoming light, limiting the entry flux while maximising the emission.[42]

The thermo-optic properties of the system are summarized in Table 5.1:

	ϵ Infrared Emissivity	α_{min} Solar Absorptivity	α_{max} Solar Absorptivity
SSM	0.76	0.10	0.16
MLI	0.77	0.32	0.49
Solar array (Solar cell face)	0.82	0.75	0.85
Solar array (back face)	0.7	0.92	0.92

Table 5.1: Thermo-optic characteristics of TCS components [26]

5.1.4 Thermal Straps and Insulating Washers

The insulating washers allow the overall thermal conductive coupling between the Star Tracker Array and the payload to be lower than 0.04 W/C. These components also enable the isolation of -Z panel of the battery zone from the rest of the structure.

5.2 Design Choices

During the design of the TCS for the Jason-2 mission different possibilities were studied and thoroughly analyzed. Due to the volume constraints of the platform, the main objective of the TCS is to simply satisfy thermal requirements despite an equipment layout not necessarily optimized from a thermal point of view. In this paragraph the main motivations for the choices made in the design will be highlighted and further explored. [42]

5.2.1 Constraints

Even though the subsystem is not fully optimized thermally some critical constraints must be respected in order for the subsystem to function nominally. This constraints can be summarized in the following list:

- The battery must be positioned on the Anti-Earth panel of the spacecraft;
- The propulsion zone must be located near the launcher adaptor, which is strongly affected by solar incident fluxes in some satellite modes;
- The Data Handling Unit (DHU) must be located on the Earth-pointing panel of the spacecraft, which is the least efficient for heat rejection capability;
- There does not exist any possibility to conductively uncouple the launcher adaptor from the rest of the platform and to protect it from solar fluxes.[42]

5.2.2 Requirements and Objectives

The PROTEUS Thermal Control System has been designed obeying these following general guidelines: [42]

- The passive thermal control is sized to obtain the maximum authorized temperature on the equipments in the hottest case between all phases.
- The active thermal control is sized to withstand the coldest case between all phases.

This allows to minimize the heating power demand for the coldest case in all satellite modes and to effectively ensure the limit temperatures, considering margins.

When designing the TCS specifically for the Jason-2 some objectives were selected in order to limit the changes that could be done from the original general PROTEUS subsystem design. These objectives can be summarized in the following list: [42]



Fig. 5.4: Silvered SSM on Jason 2

- No significant concept modifications must be done, such as radiators location on the spacecraft.
- No modifications in size and design of heater line components must be done in order to maintain compatibility with the PROTEUS platform.
- Only minor adaptations of thermal control components are allowed, such as a changes of the areas covered by MLI or the removal of distinct temperature sensors.

5.3 Environment and Temperature Range

Before proceeding with the reverse sizing, it is crucial to define the environmental conditions, understand the worst-case scenarios, both in the hot and cold cases, and determine the temperature ranges allowed by each system.

5.3.1 Environment

All spacecraft components have a range of allowed temperatures that must be maintained to meet survival and operational requirements during all mission phases. The spacecraft heat exchanges with the environment are shown in Figure 5.5.

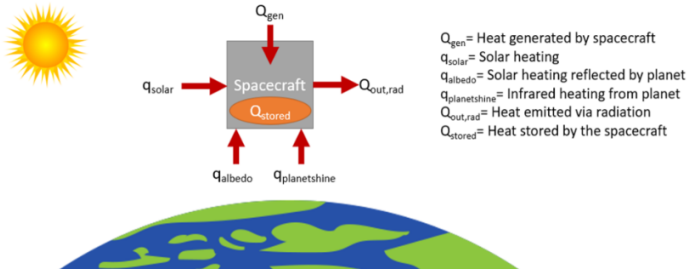


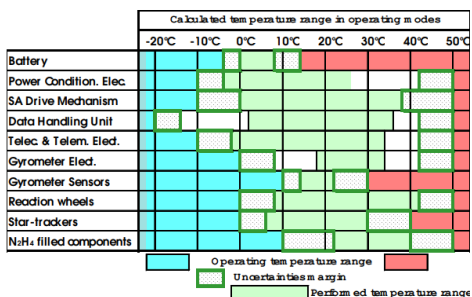
Fig. 5.5: Heat Exchanges between the Environment and the Spacecraft.

In order to dimension the system for any possible scenario, the two potential worst-case scenarios have been considered:

- **Hot Case:** The satellite is currently operating in nominal mode, with internal power consumption at its highest. Furthermore, it is in the sun's field of view, necessitating consideration for all three types of radiation.
- **Cold Case:** During an eclipse, the satellite is only exposed to infrared radiation since it is hidden by the Earth's shadow. Additionally, the spacecraft is assumed to operate in Safe Hold Mode, signifying minimal internal energy consumption and consequently reduced heat production.

5.3.2 Temperature Ranges

The platform's thermal control system aims to keep all the equipment inside their specific temperature ranges. Below are two tables outlining the temperature requirements for both the platform and the scientific payload Thermal Control System. As shown in the tables the components with the most pressing requirements belong to PROTEUS, so the critical hot temperature is assumed to be 30°C while the critical cold temperature is assumed as 0°C . These temperature take into account the acceptable ranges of all the components excluding the batteries and the attitude sensors, since these components are thermally decoupled from the rest of the system.



Instrument	Lower [°C]	Upper [°C]
T2L2 [8]	-40	40
POSEIDON [7]	-5	35
DORIS [31]	-5	5
AMR [47]	-270.5	477

Fig. 5.7: Payload Instruments' Temperature Ranges

Fig. 5.6: Proteus Platform's Temperature Ranges [42]

5.4 Reverse Sizing

Once the range of operative temperatures has been defined the reverse sizing is completed in order to size the thermal controls components, which are the heaters and the radiators. A first approximation of the sizing has been done considering a single-node model in steady-state conditions.

5.4.1 Thermal heat sources

As shown earlier, the main external sources of heat affecting the satellite are the solar, albedo, and infrared fluxes. The solar flux can be modelled as:

$$q_{solar}(r_{sc}) = q_0 \left(\frac{r_{Earth}}{r_{sc}} \right)^2 \left[\frac{W}{m^2} \right] \quad (5.1)$$

where $q_0 = 1367.5 \text{ W/m}^2$ is the solar flux at 1 AU and r_{sc} is the distance of the spacecraft from the Sun. The albedo flux has been modelled as:

$$q_{albedo} = q_{solar} \cdot a \cdot \cos(\theta) \left(\frac{R_{Earth}}{R_{orbit}} \right)^2 \left[\frac{W}{m^2} \right] \quad (5.2)$$

where $a = 0.3$ is the albedo factor of Earth [26]; θ is the irradiance angle between the normal of the panel considered and the Earth and has been assumed 0 to account for the worst-case scenario. The infrared flux is modelled as:

$$q_{IR} = \sigma \cdot \varepsilon_{Earth} \cdot T_{Earth}^4 \left(\frac{R_{Earth}}{R_{orbit}} \right)^2 \left[\frac{W}{m^2} \right] \quad (5.3)$$

where ε_{Earth} is the emissivity of the planet and T_{Earth} is the temperature of Earth, which radiates like a black body at an equivalent temperature of 255K [26].

5.4.2 Spacecraft Modelling

The spacecraft has been modelled as a single-node. The emissivity of each panel has been assumed to be equal to the -Z surface, as it is the only one in which the radiators are not included in the value. The main body areas and optical properties of each panel are summarised in Table 5.2.

Surface	Area[m ²]	Emissivity	Absorptivity
-X	0.783	0.017	0.013
+X	0.783	0.017	0
-Y	2.040	0.017	0.043
+Y	2.040	0.017	0.037
-Z	3.105	0.017	0.002
+Z	3.105	0.017	0.334

Table 5.2: Areas and thermo-optic values of the main body[6]

The radiative power of the sources can be calculated as:

$$\begin{cases} Q_{solar} = A\alpha_{sc} q_{solar} \\ Q_{albedo} = A\alpha_{sc} q_{albedo} \\ Q_{IR} = A\varepsilon_{sc} q_{IR} \end{cases} \quad [W] \quad (5.4)$$

where α_{sc} and ε_{sc} are the absorptivity and the emissivity coefficients related to the surface.

The model used considers surface +Z pointed towards Earth and for this reason, it will be the surface used to compute the heat power due to albedo and infrared fluxes, while surface -X is used to calculate the solar flux as it is considered the worst-case scenario. Surfaces +Y and -Y are perpendicular to the solar panels and for this reason, these surfaces will never point towards the Sun. Conversely, the heat emitted by the spacecraft through radiation can be divided into:

$$\begin{cases} Q_{em} = \sigma\varepsilon A_{sc} (T_{sc}^4 - T_{space}^4) [W] \\ Q_{rad} = \sigma\varepsilon A_{rad} (T_{sc}^4 - T_{space}^4) [W] \end{cases} \quad (5.5)$$

where Q_{em} is the heat emitted by all the surfaces, the total amount is given by their sum while Q_{rad} is the heat emitted by the radiators. Since the radiators are directly positioned on the spacecraft surface (mainly on $\pm Y$ axis[15]) the total surface will be reduced accordingly iteratively, $A_{sc,new} = A_{sc,tot} - A_{rad}$.

Satellite Hot Case

In the hot case all possible heat sources are considered and the satellite is in full operation so the internal power consumption is at its maximum and it is the sum of the heat dissipated by the PROTEUS and the payload[26].

$$Q_{solar} + Q_{albedo} + Q_{IR} + Q_{int,max} = Q_{em} + Q_{rad,hot} \quad (5.6)$$

The hot case occurs when the satellite is in orbit, in nominal mode, during the solar phase. The total thermal power exchanged is resumed in the following table, divided in its components.

Incoming				Outgoing
$Q_{solar}[W]$	$Q_{albedo}[W]$	$Q_{IR}[W]$	$Q_{int,max}[W]$	$Q_{em}[W]$
13.92	290.85	12.695	550	96.52

Table 5.3: Heat fluxes in the hot case

From Equation 5.6 the heat flux dissipated by the radiators can be found, $Q_{rad,hot} = 770.95W$ which correspond to a total surface for the radiators of $2.12m^2$. This value is satisfactory since it is quite close to the real one which is $2.08m^2$ [15]. Given a density area of 8 kg/m^2 , the total mass of the radiators would be 16.96 kg .

Satellite Cold Case

In the cold case only the infrared flux is present since the satellite is in eclipse phase and it is in SHM so the dissipated internal power by the platform is lower[26] and the payload is not active.

$$Q_{IR} + Q_{int,min} + Q_{heaters} = Q_{em} + Q_{rad,cold} \quad (5.7)$$

In this equation the only unknown is the heat that must be produced by the heaters in order not to go below the minimum acceptable temperature. The heat components are resumed in Table 5.4

Incoming		Outgoing	
$Q_{IR}[W]$	$Q_{int,min}[W]$	$Q_{em}[W]$	$Q_{rad,cold}[W]$
12.695	180	63.62	508.16

Table 5.4: Heat fluxes in the cold case

The heat required by the heaters through this equation should be $379.08W$, which is quite large. This is probably due to how the problem was modelled, since the spacecraft is considered as single-node and it does not take into consideration that different parts of the satellite require different amount of heat: only the critical components need to be kept hot while most of the parts can go below $0^\circ C$.

Assignment 6

Electrical Power Subsystem

6.1 Architecture

The electrical power subsystem of a satellite is a critical component that ensures the satellite's functionality by generating, storing, and distributing electrical energy to all the other subsystems of the spacecraft. For Jason-2, considering its placement on a LEO, the choice of the primary energy source easily fell on a solar array, while during eclipses power will be provided by batteries, which makes them the secondary power source.

Analyzing specifically how the electrical energy is generated in the satellite, it can be noted that there are two symmetric solar arrays located near the center of mass of Jason-2 itself, each equipped with single-axis stepping motors, in order to control the orientation of each wing.

A Lithium-Ion battery is used to store the energy which is then distributed through a single unregulated primary electrical bus, which has an average voltage of 28V and can vary between 23 and 36 V depending on the state of charge of the battery.

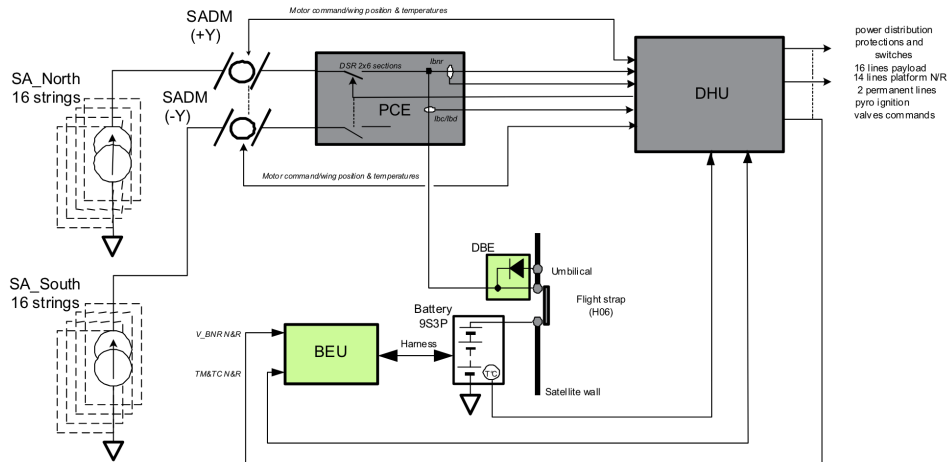


Fig. 6.1: EPS overall architecture

The average power required by the PROTEUS platform in nominal mode is 300 W while the payload average consumption is 250 W [38]. Payload power interface is given by the DHU, which typically provides 16 switchable unregulated power line on the unregulated bus, with a maximum current for each line of 5 A. This distribution permits the usage of 16 lines simultaneously or a complete cold redundancy for up to 8 lines at the time. [26]

6.1.1 EPS Components

Solar Array

The solar arrays of the Jason-2 satellite consist of 32 strings, each containing 102 standard Silicon solar cells connected in series, which are organized into 12 digital sections at the input of the Power Conditioning Equipment. The current output from each string is affected by the bus voltage, sunlight exposure, temperature, and the radiation dose received

by the cells. Covering a total area of 9.6 m^2 , the solar array is capable of delivering a maximum power of 1250 W at the beginning of its operational life (Beginning of Life (BOL)).

The orientation in space of the SA is regulated by the Solar Array Drive Mechanism (SADM), which aligns the panels using an assembly consisting of a motor and an appropriate transmission.

Power Conditioning Equipment

The PCE manages the electrical power of the solar array connecting and disconnecting the solar array cells to the bus. The number of strings connected to the bus can change from 2 to 32 by turning On and Off the electrical sections. To ensure the satellite receives the minimum required current, at least two strings are to be always kept connected. The PCE delivers the required charge current, according to the control commands coming from DHU,



Fig. 6.2: One wing of the SA on Jason-2

Battery

For the electrical functional chain of PROTEUS a single battery permanently connected to the main bus was used, and its charge is ensured by the on board software, which adjusts the number of solar sections connected to the bus.

The battery used for the platform is a 9S3P VES 100 Lithium-Ion with a capacity of 26Ah. The battery is composed of:

- 9 cell packages connected in series, where each package is made up of 3 cells in parallel to provide a nominal capacity of 78Ah.
- 9 safety devices, called Bypass, each dedicated to a cell package.
- 18 shunts, used to compensate for the dispersion of the state of charge among all the cell packs of the battery and to balance the cell packs, both the 9 nominal and the 9 redundant ones.
- 2 heaters and 3 thermistors for Battery Management (BM) thermal control.
- A harness to connect the battery to the Battery Electronic Unit (BEU).

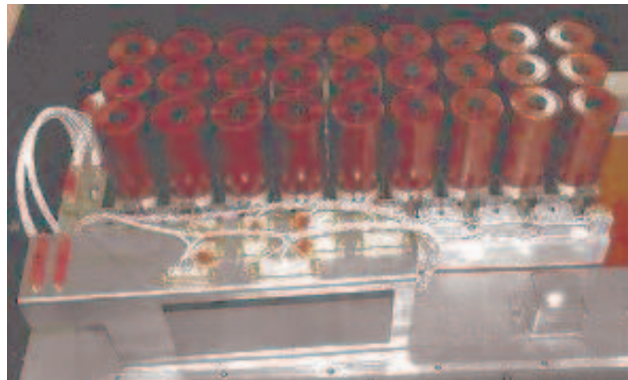


Fig. 6.3: Battery Pack on Jason 2

Battery Electronic Unit

The BEU is a crucial component that monitors and manages the voltage of individual cells in the battery. Its functions include measuring cell voltages, controlling communication between cells, activating bypasses when needed, converting primary voltage, and interfacing with other subsystems.

6.1.2 Battery Management

The battery management system of the Jason-2 satellite ensures autonomous battery charge control after each eclipse, it is performed by the On Board Software (OBSW). This system operates in two distinct modes, sequenced at a period of 1Hz.

Mode 1: Constant Current - This mode is accessed during initialization, the initial phase of battery charging, and during discharge. Its primary objective is to provide a constant current when the solar array (SA) is exposed to sunlight.

Mode 2: Constant Voltage (Tapering Mode) - This mode is activated when the maximum battery cell voltage reaches a predefined limit (adjustable up to 4.1 V). In this mode, the battery management system calculates the number of PCE sections to switch On or Off to maintain the battery voltage between two thresholds [$V_{limit} - \Delta V_{dis}$] and [V_{limit}]. If the voltage drops to an adjustable lower level, the system reverts to Mode 1 to ensure optimal battery performance and longevity.

6.2 Power Budget and phase analysis

This section will estimate the power budget needed in the Nominal Mode (NOM) for the eclipse and daylight phases, which are the two key phases. This process requires unifying all the results from the previous chapters and conducting a thorough literature analysis. Not all subsystems had a well-defined power budget, so some values were reasonably assumed, knowing the total power budget and some of the other subsystems' power budget.

	Daylight [W]	Eclipse [W]
Proteus	300	225
Propulsion	-	
TTCM	60	
ADCS	100	225
TCS	40	
OBDH	100	
Payload	250	75
POSEIDON	78	
AMR	31	
DORIS	42	
GPSP	17.5	
CARMEN-2	10	
LPT	15	
T2L2	48	
Other Systems (TCS, TTCM...)	10	40
Total	550	300
Margin +20%	+ 110	+ 60
Total Margined	660	360

Table 6.1: Power Budget Analysis

6.3 Reverse Sizing

6.3.1 Introduction

In this section of the report a preliminary sizing of the primary and secondary electrical power subsystems will be performed. This sizing will take into account the data available of the subsystems and some reasonable assumptions of everything which could not be found.

The sizing was performed at the worst possible power consumption case, both under sunlight exposure and in eclipse, applying a 20% safety margin.

Once the total power requirements are known, the primary power source may be sized. For Jason-2, the primary power source are the two solar arrays, which provide all the power for the system and for the recharging of the batteries while exposed to sunlight.

As a secondary power source, batteries were chosen to provide power to the system during the eclipse periods. A major change was performed with respect to the previous Jason-1 mission as the batteries were changed. The satellite upgraded its batteries from the previous single Nickel-Cadmium battery to a Lithium-Ion, due to their improved charging efficiencies and low leakage. [62]

Furthermore the system utilizes a quasi-regulated power system, similar to the one utilized in the Jason-1 mission. This meant that the discharge of the battery was unregulated, while the charge of the battery was regulated by the Power Conditioning Equipment (PCE) and more specifically each cell was supplied with the correct voltage through a Battery Electronic Unit (BEU). [62]

6.3.2 Establishing Initial Parameters

Before beginning the reverse sizing process, it is crucial to define key parameters in accordance with the datasheet and environmental conditions.

The environmental evaluation takes into account the satellite's performance under nominal conditions. The orbit period during this phase, is typically around 112 minutes. The duration of eclipses is then calculated using the following trigonometric formulas:

$$T_{eclipse,max} = 2 \sin \left(\frac{R_e}{R_e + h_{s/c}} \right)^{-1} \cdot \sqrt{\frac{(R_e + h_{s/c})^3}{\mu_e}} = 34.82 \text{ min} \quad (6.1)$$

Table 6.2 provides a concise summary of the environmental and system parameters:

Environmental Data		System Required Data	
Sun Irradiance	$P_0 = 1366.1 \text{ W/m}^2$	Daylight Power	$P_d = 660 \text{ W}$
Time in Eclipse	$T_e = 34.82 \text{ min}$	Eclipse Power	$P_e = 360 \text{ W}$
Time in Daylight	$T_d = 77.60 \text{ min}$	Expected Life Time	$T_{life} = 5 \text{ y}$
Inclination Angle	$\theta = 25 \text{ deg}$	Voltage	$V_{sys} = 28V$
		Daylight Efficiency	$X_d = 0.85$
		Eclipse Efficiency	$X_e = 0.65$

Table 6.2: Initial Data EPS

Another crucial aspect to consider is the expected mission's duration. Originally, the mission was envisioned for a 3-year period, however, according to the Proteus manual, sizing of the Electrical Power Subsystem for a 3-year mission with 4 solar array failures is comparable to the sizing of a 5-year mission without failures. Consequently, all reverse sizing is done based on a 5-year duration, despite the actual mission lasting nearly eleven years.

Jason-2 utilizes a Saft VES 100 battery model, with a capacity of 26 Ah chosen instead of the specified 27 Ah indicated in the datasheet [55]. This decision is consistent with findings from a study analyzing the changes destined for the EPS, following the Jason-1 mission[62]. In the same document, it's notable that a very low DOD was deliberately chosen to prevent battery degradation, given the low orbital period and high cycle count, and from our point of view, in anticipation of potential mission time extensions, as observed with Jason-1.

Although nothing was found on the solar panel cells' precise model, it was taken into account the use of a space-grade model used in that period, which had similarities with data found on other sources, such as the use of Si cells and similar absorbance and emissivity coefficients. [26]

According to the Platform manual [26], attitude control and the Solar Array Drive Mechanism (SADM) can achieve a 90% recovery of sunlight in the case of a non-sun-synchronous orbit, such as that of Jason-2. This indicates that, in the worst scenario, there will be a $\theta = 25 \text{ deg}$ between the sun and the solar panel.

Table 6.3 highlights the data of Jason-2's solar array and battery pack:

Solar Array: Spectrolab Silicon K4702 [57]		Battery: Saft VES 100 [55]	
Efficiency at BOL	$\epsilon = 0.133$	Specific Energy	$E_m = 118 \text{ Wh/kg}$
Degradation per year	$dpy = 0.028$ [39]	Density Energy	$E_v = 230 \text{ Wh/dm}^3$
Inherent Degradation	$I_d = 0.76$	Efficiency	$\mu_{batt} = 0.80$
Cell Voltage	$V_{solar,cell} = 0.585V$	DOD	$DOD = 15\%$ [62]
Cell area	8 cm^2	Cell voltage	$V_{batt,cell} = 3.6V$
		Cell Capacity	$C_{cell} = 26 \text{ Ah}$ [62]

Table 6.3: Solar Cells and Battery Data

6.3.3 Calculation and sizing

Solar array

In accordance with section 6.2, the worst-case scenarios for power consumption occurs during the nominal phase in daylight when the system is fully operational and requires charging the battery for the eclipse. The first step is to calculate the total power requested by the solar array as:

$$P_{sa} = \left(\frac{P_e T_e}{X_e T_d} + \frac{P_d}{X_d} \right) = 1025 \text{ W} \quad (6.2)$$

Then the specific power at the beginning of life is found:

$$P_{BOL} = \epsilon_{solar} P_0 I_d \cos(\theta) = 146.72 \text{ W/m}^2 \quad (6.3)$$

Then the specific power at EOL is evaluated as:

$$P_{EOL} = P_{BOL} L_{life} = 127.29 \text{W/m}^2 \quad \text{with: } L_{life} = (1 - dpy)^{T_{life}} = 0.87 \quad (6.4)$$

The surface area of the Solar Array (SA) can be calculated using the SA power requirement and the specific power output at the EOL. According to ESA standards [24], it is advisable to size the array considering at least one string failure. Considering the 8 panels (one string per panel) with 4 panels per wing, the sizing is based on 7 panels and then the eighth is added.

$$A_{SA} = \frac{P_{SA}}{P_{EOL}} = 9.08 \text{m}^2 \quad A_{panel} = A_{SA}/7 = 1.3 \text{m}^2 \quad (6.5)$$

Furthermore, the calculation of the number of cells in series needed to achieve a voltage of 28V can be straightforwardly determined, followed by the evaluation of the total number of cells required using the formula:

$$N_{series} = \text{ceil}\left(\frac{V_{sys}}{V_{cell}}\right) \quad N = \text{ceil}\left(\frac{A_{SA}}{A_{cell}}\right) \quad N_{tot} = \text{ceil}\left(\frac{N}{N_{series}}\right) N_{series} \quad (6.6)$$

Afterward, a faster recalculation is required to determine the new value following the selection of the number of cells.

$$V_{real} = N_{series} V_{cell} \quad A_{SA} = N_{tot} A_{cell} \quad (6.7)$$

Finally, it is also important to make a rough estimation of the mass. Considering a silicon layer of $200\mu\text{m}$ [58] ($\rho = 2330 \text{kg/m}^3$) and an aluminum honeycomb of 3cm ($\rho = 123 \text{kg/m}^3$) the final table can be easily compiled comparing the panel system without redundancy, the panel system with redundancy, and the actual panel mounted on Jason-2.

SOLAR ARRAY	NO Redundancy	WITH Redundancy	Jason2
N _{cell}	11376	13002	N/A
Voltage [V]	28.08	32.09	23-36 [26]
Area [m ²]	9.06	10.4	9.6 [26]
Mass [Kg]	37.82	43.23	43 [39]

Table 6.4: Solar Panel Sizing and Comparizon

It is interesting to note the different values compared to the real Jason-2 case. The difference can be attributed to the choice of solar array efficiency, which significantly affects the sizing. Another difference could be the use of ESA's redundancy guidelines, which have been in place since 2017 and surely were not followed by the Jason-2 mission, launched in 2008.

Assuming that the SA modeled in hte reverse sizing is exactly the same as the one mounted on Jason-2, the calculation without redundancy is the closest to the real scenario. The area evaluation appears plausible as it acknowledges the empty gaps between the cells, present in the real panels utilized for the Jason-2 mission, which increase the panel's actual area without adding power. Additionally, the mass evaluation seems plausible as it does not consider other components like the junctions between panels and the SADM.

Battery

During the analyzed mission, the spacecraft passed through many solar eclipse phases, necessitating a secondary power source.

The first step is to determine the battery capacity required to meet the power demand, calculated as:

$$C = \frac{T_e P_e}{(DoD) N \eta} = 1638.59 \text{ Wh} \quad (6.8)$$

where $N = 1$ is the number of battery packs and $DoD = 15\%$ is the maximum depth of discharge.

Then the number of cells in series can be evaluated as:

$$N_{series} = \text{ceil}\left(\frac{V_{sys}}{V_{cell}}\right) = 8 \quad (6.9)$$

This value must be increased according to ESA guidelines [24] from 8 to 9, in order to add redundancy, considering one string failure. It is important to note that the system has the ability to bypass the single string. Then, a new value for the bus voltage can be obtained:

$$V_{sys,new} = N_{series} V_{cell} = 28.8 \text{ V} \quad (6.10)$$

$$C_{string} = \mu_{batt} C_{cell} V_{sys,new} = 599.04 \text{ Wh} \quad (6.11)$$

where $\mu_{batt} = 0.8$ represents a typical value for the package efficiency. To achieve the desired capacity, the number of cells needed can be calculated as $N_{parallel} = \text{ceil}\left(\frac{C}{C_{string}}\right) = 3$.

Afterwards, it is important to estimate the mass and volume of the battery, which can be obtained using the values provided in the battery datasheet [55] and in Table 6.3:

$$m_{batt} = \frac{C_{batt,real}}{E_m} \quad V_{batt} = \frac{C_{batt,real}}{E_v} \quad (6.12)$$

where $C_{batt,real}$ is the real capacity of the battery and can be obtained as: $C_{batt,real} = N_{parallel} C_{string}$.

Moreover, from the datasheet, the real values for each battery can be considered for a comparison with the obtained mass and volume. Each battery has a mass of $m_{cell} = 0.81 \text{ kg}$ and dimensions of $d = 53 \text{ mm}$ in diameter and $h = 185 \text{ mm}$ in height, resulting in a total volume of $V_{cell} = 0.41 \text{ dm}^3$.

Finally, a comparison can be made between the actual data and the reverse sizing using the summary table.

BATTERY	NO Redundancy	WITH Redundancy	Jason2 [62]
Total Cell	8s-3p: tot 24	9s-3p: tot 27	9s-3p: tot 27
Capacity [Wh]	1797.12	2021.76	N/A
Max Voltage [V]	28.80	32.40	36.9
Volume [dm ³]	From E_v	7.81	29.7
	From $N_{battery}$	9.84	
Mass [Kg]	From E_m	15.23	28.4
	From $N_{battery}$	19.44	
		From E_m	17.13
		From $N_{battery}$	21.87

Table 6.5: Battery Sizing and Comparizon

As expected, the results obtained differ slightly from the actual values. The additional mass and volume account for the casing and other circuitry of the battery cell, as shown in Figure 6.3.

Assignment 7

Configuration System & On-Board Data Handling

7.1 Configuration System

In space missions, satellite configuration design plays a critical role in maximizing performance, volume, and cost-efficiency. This kind of optimization is necessary to ensure long-term missions and success.

In this section, the guiding principles behind the development of the Jason series are explored, utilizing documented sources and a reverse engineering approach. It is important to note that Jason-2 utilizes the robust Proteus platform, developed by the current Thales Alenia Space. This versatile platform is a multiplatform bus satellite designed to fulfill various missions, including COROT, SMOS, CALIPSO, and giove B, among others [49]. Furthermore, it simplifies the Jason team's design, testing, and assembly procedure to only configuring the payload with scientific instruments and verifying compatibility. This strategy saves both money and time.

In order to satisfy the technical and mission requirements, the configuration system process began with the PROTEUS documentation and continued from there [26]. To initiate the discussion, it is essential to highlight the particular requirements that guide the configuration choices:

- R1:** Nadir pointing for communication and scanning Earth
- R2:** High accuracy in Precise Orbit Determination (POD)
- R3:** High accuracy in pointing
- R4:** Constraints due to the launcher adapter of Delta II
- R5:** Symmetry and center-of-mass considerations for control
- R6:** Developing the payload based on Proteus dimensions and considerations
- R7:** Positioning of elements taking into account thermal control

For the analysis, initial considerations will focus on the launcher and the volume constraints it imposes. Following this, a straightforward design evaluation of the external distribution will be conducted, along with an analysis of the internal configuration.

7.1.1 Vehicle Shape and Interface with Launcher Fairing

The final dimensions of Jason-2 in its folded configuration are 1x1x3.7 meters [52]. According to the Proteus manual[26], a brief overview of the generic payload configuration is provided in Figure 7.1 .

As it can be seen, the satellite must develop vertically in order to meet the launcher constraint. Proteus acts as the base, supporting the entire satellite with dimensions of 0.945x0.945x1 meters. Ideally, the payload should match the dimensions of Proteus. However, this is not possible due to two specific components. Firstly, POSEIDON-3 has an antenna with a diameter of 1.2 meters [3], which is contained vertically within the system. Consequently, the payload dimensions become 0.945x0.945x1.28 meters. Secondly, the Advanced Microwave Radiometer (AMR), must be oriented towards the Earth to map the planet. This instrument needs to be placed at the top of the satellite because it does not have any folding mechanical parts. After accounting for the AMR's 1.5 m total height (one meter for the antenna's diameter and around 0.5 m for the supports), the overall height of the entire satellite (payload module + proteus) is 3.7 m.

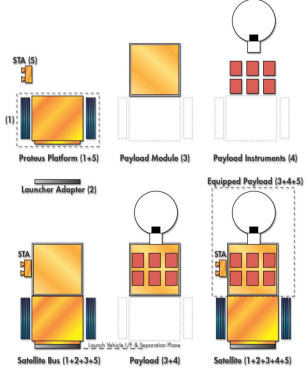


Fig. 7.1: General Satellite Architecture based on Proteus Bus



Fig. 7.2: Jason 2 Launcher Configuration

Moreover, it is necessary to verify the lateral dimensions. The worst case is not in the direction of the solar array but in the Z direction (see reference system in Figure 7.3). The communication antenna on the -Z_s panel and the Doris antenna on the +Z_s panel represent the longest points. The antennas are about 45 cm long [26], and from the various images analyzed, the Doris antenna appears to be slightly longer (50-60 cm). Therefore, in the Z_s direction, the total length is about 2 meters versus the 2.743 meters fairing of the Delta 2 [59].

7.1.2 External Surface design

To accurately describe the positioning of each satellite component, it is essential to establish a reference system. The reference system outlined in the Proteus manual will be utilized for consistency.

Requirement R1 is crucial, as it mandates the positioning of quite all instruments to face the Earth due to the satellite's nadir pointing orientation. As previously stated in section 7.1, due to spatial constraints, POSEIDON-3 occupies the entire +Z_s panel. LRA and DORIS are symmetrically placed at the base of the +Y_s and -Y_s panels, respectively, always pointing towards the Earth. This opposite placement is due to weight distribution considerations. Moreover, both instruments are mounted on a structural extension to avoid obstructing the FOV of other scientific payloads (as shown in Figure 7.4 and Figure 7.6). The AMR is positioned on the +X_s panel, with its 1 meter diameter antenna facing the Earth. Due to the nadir pointing requirement (R1), the GPSP system is mounted across the -Z_s and +X_s panels to maintain communication with GPS satellites in higher orbits, which are part of the mission's space segment. In some ways, this placement also satisfies Requirement R2, since the POD system requires an unhindered view. Similarly, the Star Tracker Array (STA) is placed on the back of the satellite on the -Z_s panel to ensure a clear FOV free from other systems. This careful arrangement of instruments ensures optimal functionality and adherence to mission requirements like Requirement R3.

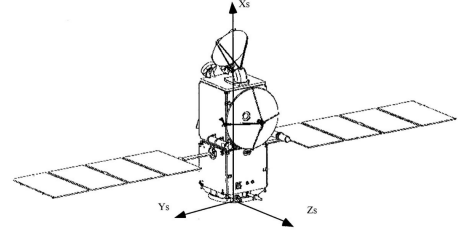


Fig. 7.3: Reference Frame of Jason 2 [26]

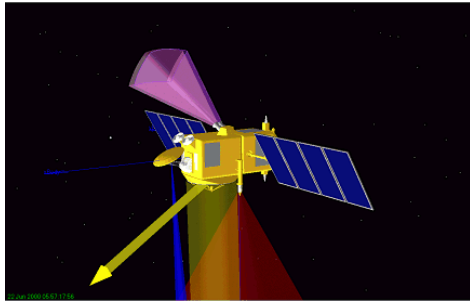


Fig. 7.4: Instrument FOV Analysis

It is now possible to inspect the Proteus platform's external components. First, consideration is given to the thruster position on the -X_s panel. By placing the thruster here, the design ensures that all thrust is applied along a single axis, simplifying the propulsion system and improving the efficiency of orbital adjustments and station-keeping maneuvers. Moreover, the +Y_s and -Y_s panels are where the SA are located. Additionally, Proteus is equipped with two antennas for Earth communication. One antenna points towards Earth, while the other, located on the opposite panel, serves as a redundant system. Final considerations can be made regarding the silvered SSM that covers most of the satellite's faces to dissipate excess heat. Notably, the SSM on the star tracker array is particularly useful for maintaining optimal operating temperatures, on single long SSM on the Star Tracker Array is particularly useful for maintaining optimal operating temperatures because it dissipates heat from the active star tracker to the inactive one [42].

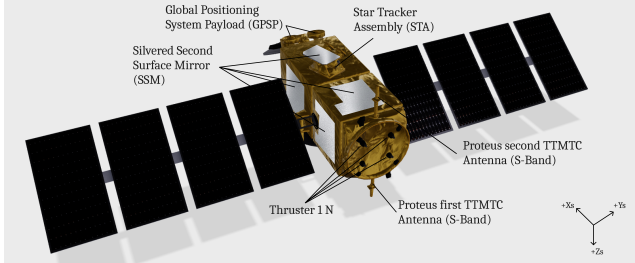


Fig. 7.5: Back View of Jason 2

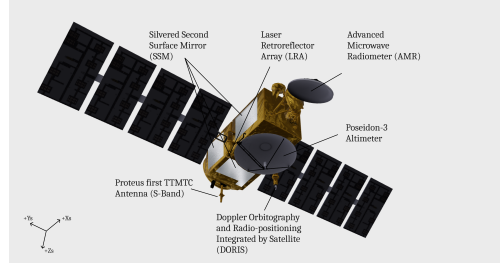


Fig. 7.6: Bottom View of Jason 2

7.1.3 Internal design

Disposition of subsystems, instruments and structures inside the satellite is critical for achieving the wanted AOCS and TCS Requirements R5 and R7. Due to the versatility, launcher and payload interfaces requirements of PROTEUS a cube geometry has been selected with the internals placed on the various dedicated internal faces.

As easily seen in Figure 7.7 and Figure 7.8 the different parts of the internals of PROTEUS have been disposed with maximum symmetry to both achieve the most geometrically centered centre of mass.



Fig. 7.7: PROTEUS's internals photo

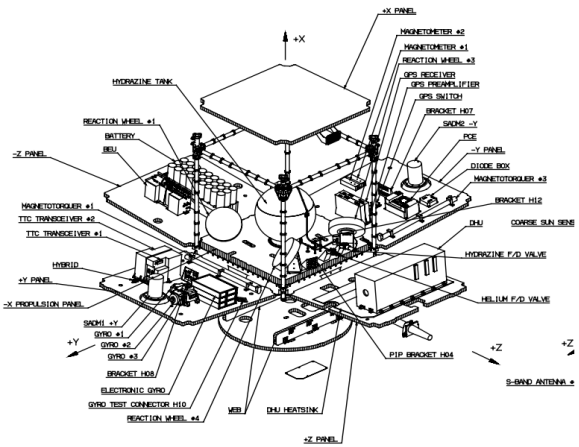


Fig. 7.8: PROTEUS internal elements

As examples: battery and DHU are big and heavy elements and so placed on opposite faces, reaction wheels are in symmetrically placed, so are the s-band antennas, and many other elements, but most importantly the hydrazine tank due to the contained 28kg of propellant. The hydrazine tank is placed in the middle most position possible, for two main reasons: one, for packing, being a sphere placed in a cube; two, for reducing to the minimum the center of mass displacement due to the reducing mass of hydrazine.

Moreover this symmetry helps to distribute heat coming from different subsystems with dedicated thermal radiators across multiple faces. Primarily the two most heat generating elements, the battery and the DHU, are placed on opposite faces with dedicated radiators.

This philosophy is also present on the payload as clearly visible in Figure 7.9, in fact the geometry is a rectangular prism with the platform coupling face of the same dimensions of PROTEUS. This geometry allows for a easy coupling with PROTEUS through four bolts placed at the vertices of the coupling face, and a hollow circular passage for all the cables and environment continuity as shown in Figure 7.10.



Fig. 7.9: Jason-2 payload internal elements

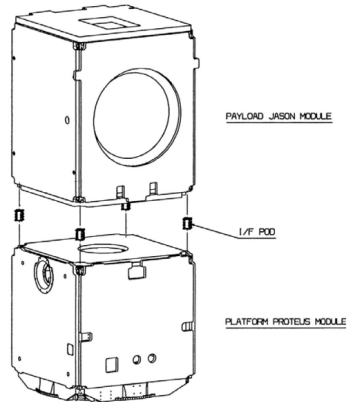


Fig. 7.10: PROTEUS interface with Jason payload

7.2 On-Board Data Handling

Acting as the satellite's brain, the On-Board Data Handling (OBDH) ensures efficient communication between subsystems, coordinates command execution, and facilitates accurate data transmission to ground stations. Its effective design is vital for the satellite's overall performance and longevity, ensuring reliable operations in the challenging environment of space. Its main functions can be resumed in:

- Satellite mode management; automatic mode transitions and routines
- Failure detection and recovery; monitoring spacecraft health and switching to SHM if necessary
- Onboard visibility; generation, maintenance and downlink of housekeeping telemetry
- Satellite command and control, consisting of management of telecommands sent by ground either to hardware or software

7.2.1 Architecture

Flight computer architecture

All of the spacecraft's computing functions are managed by the Data Handling Unit, which is centered around a computer processor known as the MA 31750. This subsystem includes 128 Kwords of 16-bit non-volatile memory, 256 Kwords of random access memory, and three gigabits of dynamic RAM mass memory[26]. It runs the Jason 2 flight software and controls the spacecraft through interface electronics. Additionally, it handles all payload data transmitted to Earth whenever the satellite is within range of a ground station. Especially for this subsystem redundancy is fundamental to reduce the risk of failure of the electronic components, that is why all units within the DHU, including the main processor, are redundant.

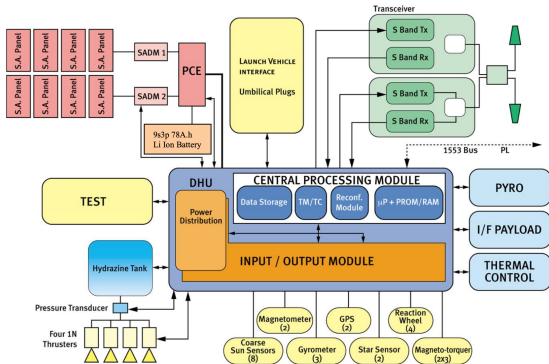


Fig. 7.11: On board computer system diagram

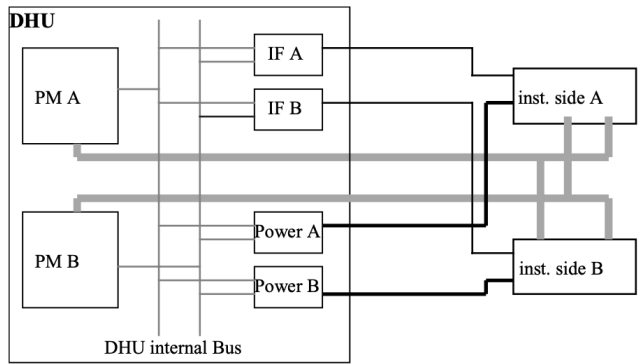


Fig. 7.12: PROTEUS interface with Jason payload

As shown in Figure 7.12 the DHU is divided into two halves, each with its own processor module, so that if one of the two halves suffers any damage, the other can continue to perform the required functions by continuously sending and managing the data received from the structure. This type of structure allows for an increase in the overall reliability of the system. The following table illustrates the concept of this redundancy, showing which elements are shared between the two halves.

	Unit	Nominal	Redundancy	Remarks
DHS	Data Handling Unit	PMA	PMB	Half Satellite
	Mass Memories	MM0, MM1, MM2, MM4	MM3 cold redundancy	Shared
TTCS	TT&C Transmitter	Tx1	Tx2	Half Satellite
	TT&C Receiver	Rx1, Rx2	1 Rx loss allowed	Hot redundancy
AOCS	GPS Receiver	GPS1 4 or more satellites 99% of the time	GPS2	Half Satellite
	Reaction Wheels	RW1 to RW4	1 RW loss allowed	Shared; no aging effects detected
	Magneto-Torques	MTB1 to MTB3 nominal coils	MTB1 to MTB3 redundant coils	Half Satellite
	SA Drive Mechanism	SADM1&2 nominal motor	SADM1&2 redundant motor	Half Satellite ; accuracy > 1%
		Potentiometer & REED relays	Potentiometer loss allowed	Shared
	Thrusters	THR1 to THR4	1 THR loss allowed	Shared (not used in NOM)
	Gyrometers	GYR1, GYR2	GYR3 cold redundancy	Shared; GYR3 checked every 6 months
	Star Trackers	STR1 Accurate>99.45% per orbit	STR2 cold redundancy	Shared; STR2 checked periodically
	Magnetometers	MAG1 No anomaly	MAG2	Half satellite (not used in NOM; checked every 6 months)
EPS	Coarse Sun Sensors	CSS1 to CSS8	1 CSS loss allowed	Shared (not used in NOM; checked every 6 months), aging effect < 2%
	Power Conditioning Electronic	12 section available	1 section loss allowed	Shared
		Nominal TM/TC	Redundant TM/TC	Half Satellite
	Battery Electronic Unit	BEU Nominal	BEU Redundant	Half Satellite
	Solar Array	32 strings of 100 cells each	4 strings loss allowed	Shared (4 strings = 1 panel section) Aging measurement is 0.75% per year versus expected 1.1%
	Battery	9 packs of 3 Lithium-ion cells	1 pack loss allowed	Shared

Table 7.1: Redundancy of main processors[20]

Payload management

The DHU manages the payload throughout the commands, offers standard thermal control, and standardized electrical interfaces (23/36V power supply, 1553 bus, specific point to point lines). A payload specific software application can be implemented in the DHU to control complex payload. The Data Handling Unit has an internal mass memory organised in two main areas :a housekeeping area to record payload and platform housekeeping data out of visibility periods and a data payload area of 2 Gbits, split in two size programmable areas to store and transmit independently payload data to ground during visibility periods. The data is transmitted from payload to mass memory through a1553 link with a maximum rate of 100 kbit/s or through a specific high speed line with a data rate up to 10 Mbit/s.

7.2.2 Reverse Sizing

The first step in correctly sizing an On-Board Data Handling subsystem is to list all the functions allocated for each subsystem. Table 7.2 collects all of the general functions used by the spacecraft, with their typical throughputs and frequencies.

It is worth noticing that all of these functions are not used simultaneously during each mode of the satellite, but to account for a worst-case scenario, the sizing is done considering all of the functions above as simultaneous.

To compute the throughput of each function, the estimation-by-similarity method is implemented, where the desired throughput is computed by comparing proportionally typical values for similar functions to the required acquisition frequency of the Jason-2 satellite.

$$KIPS = \frac{KIPS_{typ} \cdot f_{acq}}{f_{typ}} \quad (7.1)$$

As an acquisition frequency, it was assumed the use of 2 distinct frequencies: 1 Hz for secondary and non-critical

functions and 40 Hz for primary and critical functions. It was chosen 40 Hz as this is the maximum payload frequency allowed (8 Hz [26]) with a 400% margin, thus allowing control systems to act faster than the payload itself.

This process is repeated for the code and data sizes, in words per function, without having to proportionally adjust for changes in acquisition frequency.

Once these values are obtained for each allocated function, the total values for throughput, data sizes and code sizes are computed. To these values, a 400% margin is applied in order to assure an operational subsystem at all times, since typical sizes and throughput were assumed for most of the data and real values could vary significantly.

Component	Number	Typical Throughput	Typical Frequencies	Acquisition Frequencies	Throughput [KIPS]	Code Size [Kwords]	Data Size [Kwords]
Attitude Dynamics and Control Subsystem							
StarTrackers	2	2.0	0.01	1.0	200.0	2.0	15.0
Gyrometers	3	9.0	10.0	40.0	36.0	0.8	0.5
Magnetometers	2	1.0	2.0	1.0	0.5	0.2	0.1
Coarse Sun Sensors	8	1.0	1.0	1.0	1.0	0.5	0.1
Reaction Wheels	4	5.0	2.0	40.0	100.0	1.0	0.3
Magnetorquers	3	1.0	2.0	40.0	20.0	1.0	0.2
Thrusters	4	1.2	2.0	40.0	24.0	0.6	0.4
Attitude Determination	1	150.0	10.0	1.0	15.0	15.0	3.5
Attitude Control	1	60.0	10.0	40.0	240.0	24.0	4.2
Orbit Propagation	1	20.0	1.0	1.0	20.0	13.0	4.0
Complex Ephemerides	1	4.0	0.5	1.0	8.0	3.5	2.5
Error Determination	1	12.0	10.0	1.0	1.2	1.0	0.1
Propulsion Subsystem							
Pressure Sensors	5	3.0	0.1	1.0	30.0	0.8	1.5
Engine Control	1	5.0	0.1	1.0	50.0	1.2	1.5
Electrical Power Subsystem							
Solar Array Drive Mechanism	2	1.0	2.0	40.0	20.0	1.0	0.3
Power Voltage Control	1	5.0	1.0	1.0	5.0	1.2	0.5
Power Current Control	1	5.0	1.0	1.0	5.0	1.2	0.5
Power Conditioning Equipment	1	5.0	1.0	1.0	5.0	1.2	0.5
Thermal Control System							
Heaters	22	3.0	0.1	1.0	30.0	0.8	1.5
Thermistors	66	1.0	2.0	1.0	0.5	0.5	0.1
Tracking Telemetry & Telecommand Subsystem							
Uplink	1	7.0	10.0	1.0	0.7	1.0	4.0
Downlink	1	3.0	10.0	1.0	0.3	1.0	2.5
Main System Functions							
Simple Autonomy	1	1.0	1.0	1.0	1.0	2.0	1.0
Complex Autonomy	1	20.0	10.0	40.0	80.0	15.0	10.0
Fault Detection	1	15.0	5.0	40.0	120.0	4.0	1.0
Fault Correction	1	5.0	5.0	40.0	40.0	2.0	10.0
Test and Diagnostic	1	0.5	0.1	1.0	5.0	0.7	0.4
Total					1058.2	89.6	66.2
Total with margin					5291	448	331

Table 7.2: Functions allocated to the OBDH Subsystem and typical throughputs

Read-Only Memory (ROM) Computation

The Read-Only Memory is the memory allocated to store permanent (non-volatile) data.

Knowing that a word is composed by 16 bits [26], it is possible to calculate the ROM in Kilobytes as:

$$ROM = \frac{Code \cdot 16}{8 \cdot 1000} [Kb] \quad (7.2)$$

The total required ROM is obtained by summing the ROM of each function.

Random Access Memory (RAM) Computation

The Random Access Memory is the memory allocated to store the volatile data of the spacecraft.

The RAM can be computed in Kilobytes as:

$$RAM = \frac{(Code + Data) \cdot 16}{8 \cdot 1000} [Kb] \quad (7.3)$$

The total required RAM is obtained by summing the RAM of each function.

7.2.3 Conclusions

Throughput [MIPS]	ROM [Kb]	RAM [Kb]
5.291	896	1558

Table 7.3: Final requirements for the processor

In Table 7.3 are reported the total values of ROM, RAM and Throughput required by the spacecraft. These values were obtained considering a worst case scenario in which every function is activated simultaneously.

Bibliography

- [1] 1N Monopropellant Hydrazine Thruster.
<https://www.space-propulsion.com/spacecraft-propulsion/1n-hydrazine-thruster.html>.
- [2] ASF Enterprise Ground Station.
<https://ASF.alaska.edu/asf-enterprise-ground-station/>.
- [3] AVISO altimetry Jason-2.
<https://www.aviso.altimetry.fr/en/missions/past-missions/jason-2.html>.
- [4] Climate Data on Fairbanks, USA.
<https://en.climate-data.org/united-states-of-america/alaska/fairbanks-1403/>.
- [5] Doris - Documents for the data analysis.
<https://ids-doris.org/analysis-documents.html>.
- [6] DORIS satellites models implemented in POE processing.
<https://ids-doris.org/documents/BC/satellites/DORISSatelliteModels.pdf>.
- [7] eoPortal Jason-1.
<https://www.eoportal.org/satellite-missions/jason-1>.
- [8] eoPortal Jason-2.
<https://www.eoportal.org/satellite-missions/jason-2>.
- [9] eoPortal Jason-3.
<https://www.eoportal.org/satellite-missions/jason-3>.
- [10] EUMETSAT, Collecting the data.
<https://www.eumetsat.int/collecting-data>.
- [11] ICSO 1997 - A new European small platform: Proteus and prospected optical application missions .
- [12] MathWorks, Documetation .
<https://it.mathworks.com/help/satcom/ref/slantrangecircularorbit.html>.
- [13] Multi Layer Insulation Overview.
<https://www.dunmore.com/products/multi-layer-films.html>.
- [14] NOAA's Wallop and Fairbank CDAS website.
<https://www.nesdis.noaa.gov/about/our-offices/fairbanks-command-and-data-acquisition-station-fcdas>.
- [15] Preliminary Strategy For Jason-2 Pod.
https://ids-doris.org/documents/report/AWG200806/IDSAWG0806_LCerri_Jason2PODStrategy.pdf.
- [16] Rafael space propulsion catalogue.
<https://www.rafael.co.il/wp-content/RAFAEL-SPACE-PROPULSION-2021-CATALOGUE-2.pdf>.
- [17] Rsi 45 momentum and reaction wheels 15 – 45 nms with integrated wheel drive electronics.
<https://satcatalog.s3.amazonaws.com/components/199/SatCatalog-Collins-Aerospace-RSI-15-215-20-Datasheet.pdf>.
- [18] RUAG's S-Band TTC Antennas Data Sheet.
<https://spacesupplier.ir/wp-content/Catalog-S-band-TTC-Antennas.pdf>.
- [19] Spacecraft bus.
<https://proteus.cnes.fr/en/PROTEUS/platform.htm>.
- [20] SpaceOps2014, Jason1 Paper .
<https://arc.aiaa.org/doi/pdf/10.2514/6.2014-1609>.
- [21] State-of-the-Art of Small Spacecraft Technology, 7.0 Thermal Control.
<https://www.nasa.gov/smallsat-institute/sst-soa/thermal-control/7.3.11>.
- [22] Ti 6al 4v (grade 5) titanium alloy data sheet.
<https://kyocera-sgstool.co.uk/titanium-resources/ti-6al-4v-grade-5-titanium-alloy-data-sheet/>.
- [23] Wallops Command and Data Acquisition Station.
<https://www.ospo.noaa.gov/Operations/WCDAS/>.

- [24] ESA. Concurrent design facility studies standard margin philosophy description, 2017.
- [25] NASA. Ocean Surface Topography Mission/ Jason 2 Launch - Press Kit/JUNE 2008.
<https://sealevel.jpl.nasa.gov/internal-resources/389/>.
- [26] NASA & Alcatel. PROTEUS User's Manual, 2004.
- [27] Adcole Maryland Aerospace. Coarse Sun Sensor Datasheet.
<https://satcatalog/SatCatalog-Adcole-Maryland-Aerospace-Coarse-Sun-Sensor-Pyramid-Type-Datasheet.pdf>.
- [28] A. Ambroze, M. Tomlinson, and G. Wade. Magnitude modulation for small satellite earth terminals using qpsk and oqpsk. pages 2099 – 2103 vol.3, 06 2003.
- [29] Aviso. Calibration Campaign Contribution.
<https://www.aviso.altimetry.fr/calval/absolute-calibration/corsica-calibration-sites.html>.
- [30] Aviso, NASA, NOAA and JPL. Harvest Altimetry Calibration.
<https://www.aviso.altimetry.fr/0220Haines20harvest2011.pdf>.
- [31] Alexandre Belli, P. Exertier, Etienne Samain, Clément Courde, Francois Vernotte, C. Jayles, and A. Auriol. Temperature, Radiation and Aging Analysis of the DORIS Ultra Stable Oscillator by means of the Time Transfer by Laser Link Experiment on Jason-2. *Advances in Space Research*, 58, 11 2015.
- [32] Pradeep Bhandari. Robust Thermal Control of Propulsion Lines for Space Missions. Technical report, Jet Propulsion Laboratory, California Institute of Technology, 2016.
- [33] CNES C. Marechal. Jason-2 Project Status, 2018.
<https://ostst.aviso.altimetry.fr/fileadmin/OPEN-03-Marechal.pdf>.
- [34] C. Marechal, CNES. Jason-2 Project Status, 2019.
<https://ostst.aviso.altimetry.fr/OSTST2019/J2StatusMarechalv3.0.pdf>.
- [35] Rémi Canton and Pierre Pélichenko. Jason-1 (nasa-jpl/cnes) : A successful operational story throughout hardware ageing. Technical report, CNES – Centre National d'Etudes Spatiales, Toulouse, France, 2014.
- [36] Hyunwoo Cho and Kim. Concatenated schemes of reed-solomon and convolutional codes for gnss. In *2019 International Conference on Information and Communication Technology Convergence (ICTC)*, pages 338–339, 2019.
- [37] CLS & CNES. Jason-2 validation and cross calibration activities (End of mission 2019), 2022.
<https://www.aviso.altimetry.fr/fileadmin/documents/calval/validation-report/J2.pdf>.
- [38] CLS, CNES, NASA & EUMETSAT. OSTM/Jason-2 Product Handbook, 2011.
<https://www.ospo.noaa.gov/Products/documents/J2-handbook.pdf>.
- [39] Jean-Michel Cresp, Eric Boutelet, Jean Massot, and Pierre Tastet. Proteus Electrical Functional Chain: Flight Return Experience. In *9th European Space Power Conference*, volume 690 of *ESA Special Publication*, page 127, October 2011.
- [40] D. Li, G. Creamer. Attitude Control Subsystem (ACS) Training, January 2001.
<https://hesperia.gsfc.nasa.gov/rhessi3/docs/official-docs/RHESSI-Documentation/Training/ACS-training.pdf>.
- [41] L. King F. Gulczinsk III, C. Hall. High Power Orbit Transfer Vehicle . Technical report, Air Force Research Laboratory, July 2003.
<https://www.researchgate.net/publication/235057840-High-Power-Orbit-Transfer-Vehicle>.
- [42] "Francis Arbusti, Joel Gayrard". "The Thermal Control Design and Test Philosophy of the Proteus Platform", 1999.
<https://www.sae.org/publications/technical-papers/content/1999-01-2087/>.
- [43] CNES G. Zaouche. OSTM/Jason-2 Mission Overview, 2009.
<https://www.aviso.altimetry.fr/fileadmin/documents/OSTST/2009/oral/Zaouche.pdf>.
- [44] J. Perbos G. Zaouche. OSTM/Jason-2: Assessment of the System Performances (Ocean Surface Topography Mission: OSTM). *Marine Geodesy*, 33(sup1):26–52, 2010.
- [45] EUROCKOT Launch Services GmbH. Rocket User's Guide, 2011.
<https://www.eurockot.com/wpcontent/uploads/2012/10/UsersGuideIss5Rev0web.pdf>.
- [46] Ariane Space Group. Ariane 5 User's Manual, 2011.
<https://www.arianespace.com/wp-content/uploads/2011/07/Ariane5-Users-Manual-October2016.pdf>.
- [47] "Jenna L. Kloosterman, Shannon Brown". "The Advanced Microwave Radiometer – Climate Quality (AMR-C) Instrument for Sentinel-6", 2017.
<https://www.nrao.edu/meetings/isstt/papers/2017/2017000034.pdf>.
- [48] Arif Karabeyoglu. Launch Trajectories, Advanced Rocket Propulsion course of Stanford University , 2019.
<https://web.stanford.edu/cantwell/AA284A-Course-Material/Karabeyoglu.pdf>.
- [49] Gunter D. Aldquo Krebs. Thales alenia: Proteus.
https://space.skyrocket.de/doc_sat/alcatel_proteus.htm.

- [50] M. Sghedoni, J.L. Beaupellet, J. Busseuil, F. Douillet.
 Attitude and Orbit Control System for Multimission Spacecraft Platform.
Spacecraft Guidance, Navigation and Control Systems Vol. 381, page 133, February 1997.
<https://articles.adsabs.harvard.edu/cgi-bin/nph-iarticle-query?>
- [51] NASA. Jason-2 SLR System & POD Status, 2008.
<https://ilrs.gsfc.nasa.gov/docs/ja1-2-slr-pass.pdf>.
- [52] NASA. OSTM/JASON-2 Press Kit, 2008.
https://www.jpl.nasa.gov/news/press_kits/jason-2.pdf.
- [53] O'Neil. *The Merck Index - An Encyclopedia of Chemicals, Drugs, and Biologicals*.
 Royal Society of Chemistry, 2013.
- [54] Northrop Grumman Orbital. Taurus Launch System, 1999.
<http://www.georing.biz/usefull/Taurus-User-Guide.pdf>.
- [55] Saft. Rechargeable lithium battery VES 100.
https://alpha-energy.ru/D/0000009803/EB_Saft_VES_100_33017-2-0608_200806_en.pdf.
- [56] Arian Space. Soyuz User's Manual, 2012.
<https://www.arianespace.com/wp-content/uploads/2015/09/Soyuz-UsersManualMarch2012.pdf>.
- [57] Spectrolab BOEING. Silicon K4702 Solar Cells.
<https://www.spectrolab.com/DataSheets/K4702/k4702.pdf>.
- [58] Thales Alenia Space. Solar Generator Family.
https://www.thalesgroup.com/sites/default/files/database/d7/asset/document/solar_generators_family.pdf.
- [59] ULA. Delta II, Payload Planners Guide, 2007.
<https://www.ulalaunch.com/docs/default-source/rockets/deltaiiipayloadplannersguide2007.pdf>.
- [60] ULA. Wide-field Infrared Survey Explorer, 2009.
<https://www.ulalaunch.com/docs/default-source/news-items/dii-wise-mob.pdf>.
- [61] V. Couderc, G. Zaouche. Jason-3 Characteristics for POD Processing, August 2015.
<https://ids-doris.org/documents/BC/satellites/Jason-3-CharacteristicsForPODprocessing.pdf>.
- [62] V. Michoud, J. Digoin, P. Tastet, J. Loubeyre. Proteus Electrical Functional Chain: From Nichel-Cadmium to Li-Ion Battery.
<https://articles.adsabs.harvard.edu/pdf/2005ESASP.589E.106M>.
- [63] W. Lohmeyer, R. Aniceto, K. Cahoy.
 Communication satellite power amplifiers: current and future SSPA and TWTA technologies.
International Journal of Satellite Communications and Networking, 2015.
<https://core.ac.uk/download/pdf/85123635.pdf>.
- [64] J.R. Wertz, D.F. Everett, and J.J. Puschell. *Space Mission Engineering: The New SMAD*. Space technology library. Microcosm Press, 2011.
- [65] World Meteorological Organization. OSCAR (Observing Systems Capability Analysis and Review Tool).
https://space.oscar.wmo.int/satellites/view/jason_2.